ELECTRON PARAMAGNETIC RESONANCE STUDIES OF Mn^{2+} IN SOME DIA-AND PARAMAGNETIC SINGLE CRYSTALS

A Thesis Submitted
In Partial Fulfilment of the Requirements
for the Degree of
DOCTOR OF PHILOSOPHY

BY
RAMAMURTHI JANAKIRAMAN

to the

DEPARTMENT OF PHYSICS
INDIAN INSTITUTE OF TECHNOLOGY KANPUR
NOVEMBER, 1970

Certified that the work presented in the thesis has been carried out by Mr. R. Janakiraman under my supervision, and has not been submitted elsewhere for a degree.

(G.C. Upreti)
Lecturer

Department of Physics
Indian Institute of Technology
Kanpur

ACKNOWLEDGEMENTS

I wish to express my deep sense of indebtedness to Dr. G.C. Upreti for suggesting the problem and for stimulating guidance throughout. I am grateful to Prof. Putcha Venkateswarlu for his kind interest in the progress of this work.

I am thankful to Professors J. Mahanty, B.D.Nageswara Rao and T.M. Srinivasan for their interest in this work.

I have been greatly benefited by discussions with, and suggestions from, Drs. K.V. Subba Rao and M.D. Sastry, and I convey my sincere thanks to them. My thanks are due to many friends who have helped me during the course of the work, notably Dr. S.D. Pandey, Mr. V.K. Sharma, Drs. P.A. Narayana and B.V.R. Chowdari, M/s. E.V.R. Sastry, M. Mahajan and N.R. Krishna of Physics Department, and Mr. T.S. Kannan, Dr. P. Bhaskara Rao, M/s T.S. Sarma and K.S. Balachandran of Chem. Department.

I thank Mr. J.K. Misra for neat typing of the thesis, Mr. R.K. Bajpai for preparing the figures, and Mr. H.K. Panda for running the stencils.

Financial assistance from the Council of Scientific and Industrial Research, during 1968-69, is gratefully acknowledge

Finally, I take this opportunity to express my respects and regards to my parents and uncles, who have shown boundless affection and patience, and have contributed a lot to my progress.

R. Janakiraman

TABLE OF CONTENTS

LIST OF TABLES

LIST OF FIGURES

SYNOPSIS

ELECTRON PARAMAGNETIC RESONANCE STUDIES OF Mn^{2+} IN SOME DIA- AND PARAMAGNETIC SINGLE CRYSTALS

Ramamurthi Janakiraman
Ph.D.
Indian Institute of Technology, Kanpur
November, 1970

After its discovery in 1946, the study of electron paramagnetic resonance (EPR) in solids has contributed much to the information concerning the energy levels lying within few cm^{-1} from the ground state of a paramagnetic system and the various interactions in solids. The fact that the EPR spectrum is very sensitive to the symmetry and strength of the electrostatic field acting at the site of the paramagnetic system furthered its study as a structural tool. Among the paramagnetic ions of the transition group elements, divalent manganese (Mn^{2+}) has been most widely studied because of its obvious advantages over other paramagnetic ions. The thesis describes the EPR studies of Mn^{2+} in single crystals of zinc acetate dihydrate $[Zn(CH_3COO)_2 \cdot 2H_2O]$, ferrous ammonium sulfate hexahydrate $[Fe(NH_4)_2(SO_4)_2 \cdot 6H_2O]$, nickel acetate tetrahydrate $[Ni(CH_3COO)_2 \cdot 4H_2O]$, nickel sulfate heptahydrate ($NiSO_4 \cdot 7H_2O$), and magnesium sulfate heptahydrate ($MgSO_4 \cdot 7H_2O$).

The first chapter is a general introduction to the

consists of a brief summary of the phenomenon of EPR, the various electronic systems which can be studied by EPR, and the information that can be extracted from this study.This is followed by a chapter on the theory of EPR, consisting of the general theory of EPR, the crystal-field effects, and the spin-Hamiltonian formalism. These are restricted to the iron group transition elements in general, and in a few cases to Mn^{2+} in particular. A brief summary, of the fine structure of Mn^{2+}, the spin-spin and spin-lattice interactions, and the EPR of Mn^{2+} in paramagnetic single crystals, is also contained in this chapter. Under the heading 'Experimental Details' Chapter III deals with a brief sketch of the experimental setup used in the study (Varian V-4502 EPR spectrometer), a crystal rotating device used to rotate the crystal spatially inside the cavity, the simultaneous equations used in the analysis of the spectra by spin-Hamiltonian method, and a brief report on the principles of the method of linear regression used to fit the experimental data of the linewidth variation of the Mn^{2+} resonance lines with the intensity of the applied static magnetic (Zeeman) field.

Chapter IV deals with the first system taken up for study by EPR, viz., Mn^{2+} in $Zn(CH_3COO)_2 \cdot 2H_2O$. Although the unit cell of $Zn(CH_3COO)_2 \cdot 2H_2O$ is tetramolecular, the magnetic equivalency of all the four Zn^{2+} ions results in the observa-

has been the reason in taking up this system to make a beginning into the subject and to familiarise with the experimental and spectral-analyses techniques. Besides the allowed ($\Delta M = \pm 1$, $\Delta m = 0$) transitions, hyperfine-forbidden ($\Delta M = \pm 1$, $\Delta m = \pm 1$) transitions have also been observed, which made it possible to compute the quadrupole interaction constants in the spin Hamiltonian.

The primary interest in taking up the present project has been the study of EPR of Mn^{2+} in certain paramagnetic single crystals of Fe^{2+}, Ni^{2+}, and Co^{2+}, and to investigate the effect of these ions on the EPR of Mn^{2+}. These paramagnetic ions (Fe^{2+}, Ni^{2+}, and Co^{2+}) usually do not exhibit EPR at room temperature ($\sim 300^{\circ}K$) and at X-band microwave frequency ($\sim$ 9.5 GHz) because, either the spin-lattice relaxation time is very short, e.g. in Fe^{2+} and Co^{2+}, or the splitting between the levels giving rise to EPR is much larger than the energy of the incident microwave field ($\sim 0.3\ cm^{-1}$), e.g. in Ni^{2+}. The present work consists of the study in single crystals of salts of Fe^{2+} and Ni^{2+}. The first system in this class was $Fe(NH_4)_2(SO_4)_2 \cdot 6H_2O$ and Chapter V describes the EPR of Mn^{2+} in this system. Fe^{2+} in $Fe(NH_4)_2(SO_4)_2 \cdot 6H_2O$, because of its very short spin-lattice relaxation time, exhibits its EPR only below $20^{\circ}K$. Till $77^{\circ}K$, the lowest temperature we studied upto, no noticeable effect of Fe^{2+} on the EPR of Mn^{2+} has been observed. $Fe(NH_4)_2(SO_4)_2 \cdot 6H_2O$, which belongs to a class of isostructural compounds

known as Tutton's salts, has not been studied in detail for its crystal structure. Although the space group and overall symmetry are same for all these Tutton's salts, different compounds may have different distances and orientations of the atoms and molecules. Hence the EPR is expected to give an idea about these factors by a comparison of the spin-Hamiltonian constants of Mn^{2+} in this system, with those of Mn^{2+} in other Tutton's salts where the crystal structure is known completely. This has been carried out for this system.

The next two chapters deal with the EPR of Mn^{2+} in single crystals of salts of Ni^{2+}. The $(3d)^8$ configuration of Ni^{2+} in an octahedral cubic field has, as its ground state, an orbital singlet. The interplay between the crystalline field of lower-than-axial symmetry and the spin-orbit coupling removes the spin degeneracy also, and hence at X-band its EPR is normally not observed. Chapter VI is about the EPR of Mn^{2+} in $Ni(CH_3COO)_2 \cdot 4H_2O$. The characteristic spectrum of Mn^{2+} has been observed with two magnetically inequivalent sites corresponding to the substitution of the Mn^{2+} at the two Ni^{2+} sites in the bimolecular unit cell. The additional features in the Mn^{2+} resonance have been a shift of the g value along the principal z axis from the corresponding value of Mn^{2+} in the isostructural, diamagnetic $Mg(CH_3COO)_2 \cdot 4H_2O$, and a regular increase of the linewidth of the Mn^{2+} resonance lines with the intensity of the Zeeman field. These have been explained

in terms of a local magnetic field at the Mn^{2+} sites by Ni^{2+} due to the polarization effect of the Zeeman field, and the frequency dependence of Ni^{2+} spin fluctuation at room temperature - for the case where the crystalline field splitting of the Ni^{2+} ground state spin triplet is larger than the Zeeman interaction, respectively.

Chapter VII describes the EPR study of Mn^{2+} in $NiSO_4 \cdot 7H_2O$ and $MgSO_4 \cdot 7H_2O$. Here again the EPR of Mn^{2+} exhibited the characteristic magnetic inequivalency corresponding to the substitution of Mn^{2+} at the four divalent cation positions in the tetramolecular $NiSO_4 \cdot 7H_2O$ and $MgSO_4 \cdot 7H_2O$. In addition, for the system Mn^{2+} in $NiSO_4 \cdot 7H_2O$, a g-shift and the linewidth variation of Mn^{2+} resonance lines with the intensity of the Zeeman field have been observed. The g-shift is obtained in comparison with the corresponding parameter in the EPR of Mn^{2+} in isostructural, diamagnetic $MgSO_4 \cdot 7H_2O$.

At the end, an Appendix is given describing briefly the theory concerning the effect of Ni^{2+} diluting ions on the EPR of Mn^{2+}.

Each chapter is written as to be self-contained and as such repetitions of some statements became unavoidable. At the end of each chapter a list of references is given. A great deal of the contents of Chapters I and II has been gathered from certain review articles and text books. These are given as

'General References' and are not directly referred to, by a reference number, in the text. The names of the journals are abbreviated in accordance with the 'World List of Scientific Periodicals', IV Edn. Butterworths, London (1963).

CHAPTER I

INTRODUCTION

Abstract

A brief introduction is given to the phenomenon of electron paramagnetic resonance. A list of the electronic systems that can be studied by this method and the results one can obtain from this study are also given.

The great progress in microwave engineering on one hand, and the discovery of very valuable application of paramagnetic resonance method to the solution of certain problems in solid state physics, chemistry, on the other, gave a great impetus to the study of the field of electron paramagnetic resonance (EPR). EPR is the resonance absorption of microwave radiation, usually between the ground state energy levels of an electronic system, under the application of an applied static magnetic (Zeeman) field. Paramagnetic resonance can be observed in systems possessing permanent magnetic dipoles.

The Phenomenon of EPR:

The basic phenomenon of EPR can be understood by considering a single electron with spin only angular momentum $\vec{S} = 1/2$. The magnetic moment associated with this spin is given by

$$\vec{\mu} = -g(|e|\hbar/2mc)\vec{S}$$

$$= -g\beta\vec{S}, \qquad (I.1)$$

where g is the Lande g factor (2.0023 for spin only angular momentum) and β is the Bohr magneton. When this electron is placed in a Zeeman field $\vec{H}$, the two-fold degeneracy is lifted by the interaction of the magnetic moment $\vec{\mu}$ with the Zeeman field $\vec{H}$. This interaction energy is given by

$$E = -\vec{\mu}\cdot\vec{H}. \qquad (I.2)$$

If we consider the direction of $\vec{H}$ as the z axis, the two energy levels are given by

$$E_{\pm} = g\beta H_z S_z, \quad S_z = \pm 1/2. \tag{I.3}$$

In addition to the Zeeman field H_z, if a weak magnetic field rotating with a frequency ν of amplitude $H_1 \cos 2\pi\nu t$ is applied perpendicular to H_z, magnetic dipole ($\Delta S_z = \pm 1$) transitions are induced between these levels. When the frequency ν is varied continuously, at a particular frequency $\nu = \nu_o$ absorption of energy of quantum $h\nu_o$ takes place between the levels, such that

$$\begin{aligned} h\nu_o &= E_+ - E_- \\ &= g\beta H_z. \end{aligned} \tag{I.4}$$

This is illustrated in Fig. I-1. Classically speaking, resonance occurs when the frequency of radiation ν equals the Larmor precessional frequency of the spin in the field H_z. Though the transitions $E_+ \rightarrow E_-$ and $E_- \rightarrow E_+$ have the same induced probability, the larger number of spins in the lower state, because of the thermodynamical distribution, results in a net absorption.

Deviations from this picture of resonance occur in the experimental techniques adopted. Firstly, in practice it has been found more convenient to keep the frequency ν fixed and vary the intensity of the Zeeman field. Then resonance occurs at a particular $H = H_o$ such that

$$g\beta H_o = h\nu. \tag{I.5}$$

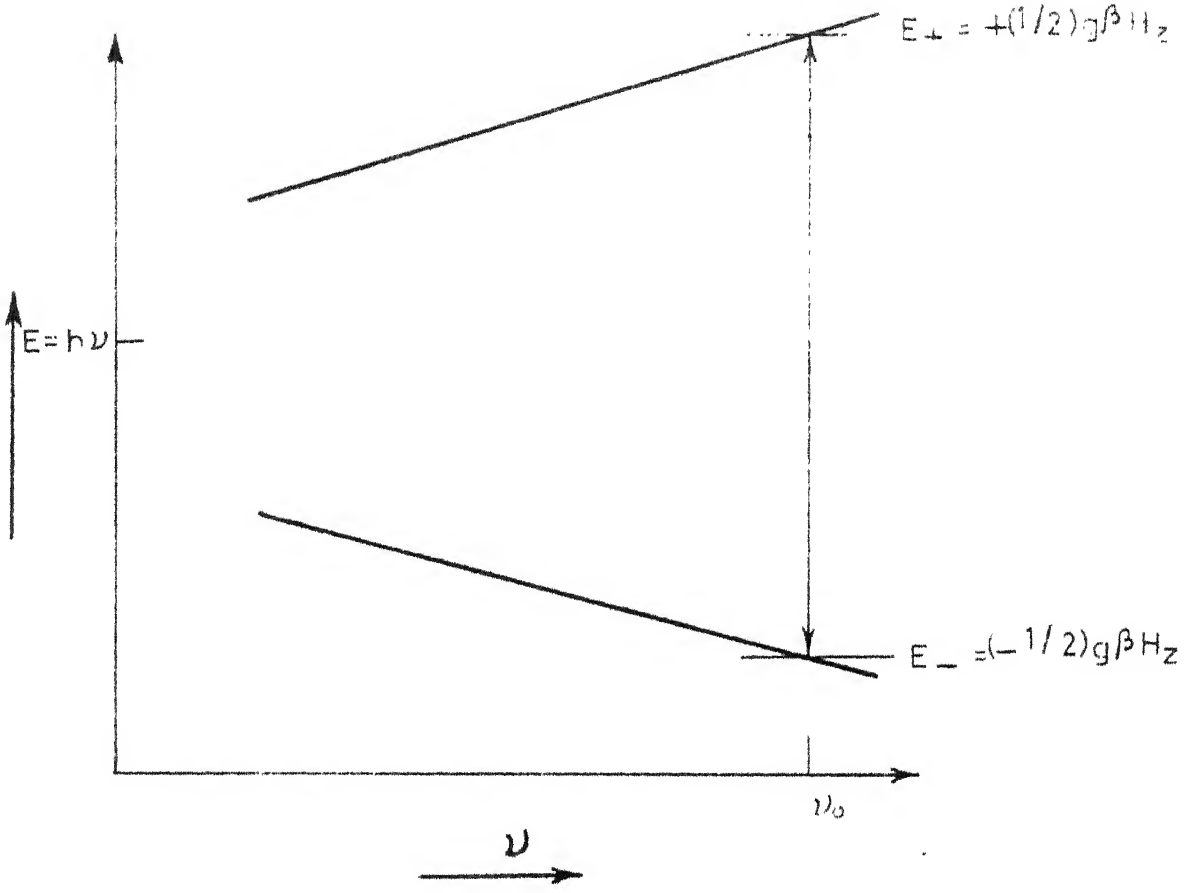

Fig. I-1 Frequency scanning at a fixed Zeeman field H_z, and the absorption of microwave radiation at frequency ν_0 corresponding to an energy $h\nu_0 = E_+ - E_-$.

Also, instead of a rotating field of frequency ν, an oscillating field of the same frequency is applied. This is because an oscillating field is equivalent to two rotating fields in opposite directions (frequencies ν and $-\nu$) and the effect of the rotating field of frequency $-\nu$ is negligibly small as it is constantly changing phase with the precessional motion.

Electronic Systems Which Exhibit EPR:

EPR can be observed in electronic systems which have non-zero resultant angular momentum. These are,

(a) atoms having an odd number of electrons, like nitrogen atom,

(b) molecules with resultant non-zero ground state angular momentum, like NO, O_2,

(c) free radicals, like CH_3,

(d) color centers produced in solids, like the F centers,

(e) metals because of conduction electrons, and

(f) ions of the transition group elements.

Results That Can be Obtained From EPR Studies:

EPR has been most widely studied in solids, especially in single crystals because of the useful information that can be obtained from the single crystal study. The concept of 'diluting' a paramagnetic complex in an isostructural diamagnetic medium[1,2] and of forming mixed crystals with diamagnetic compounds,[3] enhanced to a great extent the details obtained by

paramagnetic resonance studies (like the observation of fine-structure and hyperfine structure interactions). The discovery of EPR was followed by an extensive study at Clarendon Laboratory, Oxford, in both experimental and theoretical aspects. The experimental study has been a very valuable source of information, and on the theoretical side important ideas, like the spin-Hamiltonian formalism, were introduced.

The single crystal EPR studies of a paramagnetic complex have given valuable information regarding its spectroscopic properties and about the interactions affecting its resonance characteristics. Some of them are listed hereunder.

(a) EPR studies give accurate magnitude of the levels separated by few cm^{-1} from the ground state (falling within the energy of the incident microwave field) at room temperature ($\sim 300^{\circ}K$) itself. The study of these levels by susceptibility measurements requires experimentation at very low temperatures (near liquid helium temperatures, corresponding to $kT \sim 1\ cm^{-1}$).

(b) The decrease in the interactions between the paramagnetic complexes, by diluting in a diamagnetic compound, has increased the details obtained by EPR studies. Thus the fine, hyperfine and superhyperfine interactions of the paramagnetic complex can be studied. EPR is one direct method of finding the magnitude of nuclear spin in its ground state. The study of hyperfine structure led to the formulation of configuration mixing.[4] Sometimes the interaction of the quadrupole moment

of the nucleus with the electric field gradient can be evaluated by EPR.

(c) The sensitivity of the observed EPR spectrum to the symmetry and strength of the electrostatic field at the site of the paramagnetic complex provides useful information regarding the positions of the paramagnetic complexes in single crystals, the number of preferential and 'magnetically inequivalent' sites for a given complex in a given crystal, the point group symmetry in certain cases, and the occurrence of phase and structural transitions.

(d) The accurate g values contribute in estimating the interaction with high lying levels, the nature of chemical bonding,[5] and the magnetic effects of paramagnetic host ions.

(e) The existence of covalent bonding can be directly observed in EPR as a superstructure on the EPR transitions.[5] Covalent bonding also leads to a reduction in the strength of hyperfine interaction.[6]

(f) Finally, the various interactions contributing to the linewidth of the EPR transitions, like the spin-spin and spin-lattice interactions, can be studied.

REFERENCES

1. R.P. Penrose, Nature (London) 165, 991 (1949).
2. B. Bleaney and D.J.E. Ingram, ibid. 164, 116 (1949).
3. B. Bleaney and D.J.E. Ingram, Proc. phys. Soc. (London) A63, 408 (1950).
4. A. Abragam, Phys. Rev. 79, 534 (1950).
5. J.H.E. Griffiths, J. Owen, and I.M. Ward, Proc. Roy. Soc. (London) A219, 526 (1953).
6. J.S. van Wieringen, Discuss. Faraday Soc. 19, 118 (1955).

GENERAL REFERENCES

1. B. Bleaney and K.W.H. Stevens, in 'Reports on Progress in Physics' (Ed. A.C. Stickland) Vol. 16, p. 108. Published by the Physical Society, London (1953).
2. K.D. Bowers and J. Owen, ibid. Vol. 18, p. 304. (1955).
3. W. Low, 'Paramagnetic Resonance in Solids', Academic Press, New York (1960).

CHAPTER II

THEORY OF ELECTRON PARAMAGNETIC RESONANCE OF IRON GROUP IONS

Abstract

A brief theory of electron paramagnetic resonance is given. The crystal-field effects are included and the spin-Hamiltonian formalism is elaborated. These are restricted to the iron group transition elements in general, and in a few cases to Mn^{2+} in particular. A brief summary, of the fine structure of Mn^{2+}, the spin-spin and spin-lattice interactions, and the resonance of Mn^{2+} in paramagnetic single crystals, is also given.

Introduction:

The application of the method of paramagnetic resonance and the development of the associated crystal-field theory have led to a good understanding of the magnetic properties of ionic compounds. Of these, considerable amount of work has been done in iron group and rare earth group ions of the transition elements.

The phenomenon of electron paramagnetic resonance as exemplified by an electron with spin only angular momentum has been described in Chapter I. But in general, instead of a spin only angular momentum, one observes both the spin and orbital angular momenta affecting the EPR, and also, more often than not, one studies the EPR of a system of electrons instead of a single electron. Thus the characteristics of the electronic systems vary very widely, although the condition for resonance is unchanged (magnetic dipole transitions) as long as the oscillating field is kept perpendicular to the Zeeman field.

The contribution of both spin and orbital angular momenta to the magnetic moment introduces a resultant angular momentum $\vec{J} = \vec{L} + \vec{S}$ (in the Russell-Saunders coupling approximation) in the place of $\vec{S}$. This magnetic dipole of magnetic moment

$$\vec{\mu} = -g\beta\vec{J} \qquad \text{(II.1)}$$

has $2J + 1$ $(-J, -J+1, \ldots, +J)$ non-degenerate energy levels (M)

in the Zeeman field $\vec{H}$. Magnetic dipole transitions are induced satisfying the resonance condition

$$g\beta H_o = E_M - E_{M'}, \quad (M' = M \pm 1)$$
$$= h\nu . \qquad \text{(II.2)}$$

If before the application of the Zeeman field all the $2J + 1$ levels were completely degenerate, the resonance between any two adjacent M levels would take place at a single Zeeman field intensity H_o. If, on the other hand, the $(2J + 1)$-degeneracy before the application of the Zeeman field was removed partially or completely, the $2J$ ($\Delta M = \pm 1$) transitions would occur at different intensities of the Zeeman field. The intensities of these transitions are given by the square of the magnetic dipole transition probability $P_{M,M'}$, where

$$P_{M,M'} = \text{constant} \times \left[J(J+1) - MM'\right]^{1/2}, \quad M' = M \pm 1. \qquad \text{(II.3)}$$

Hence different $M \rightarrow M'$ transitions have different intensities. The two situations, one for which the $(2J + 1)$-fold degeneracy is not removed at all and the other for which it is partially removed, for the case of $\vec{J} = 3/2$, are shown in Fig. II-1.

Crystal-Field Effects:

The study of EPR has been most fruitful in solids, especially in single crystals, because of its definite advantages (as mentioned in Chapter I). In this class the most widely studied have been the atoms of the transition elements,

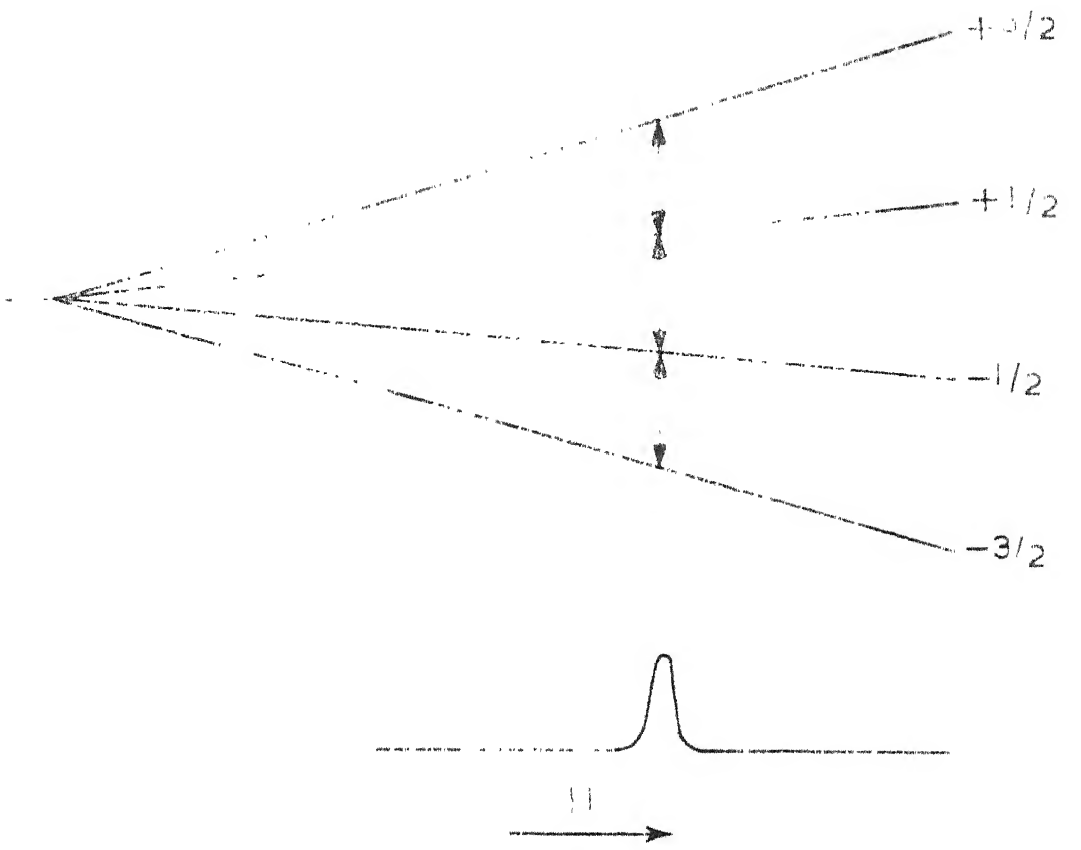

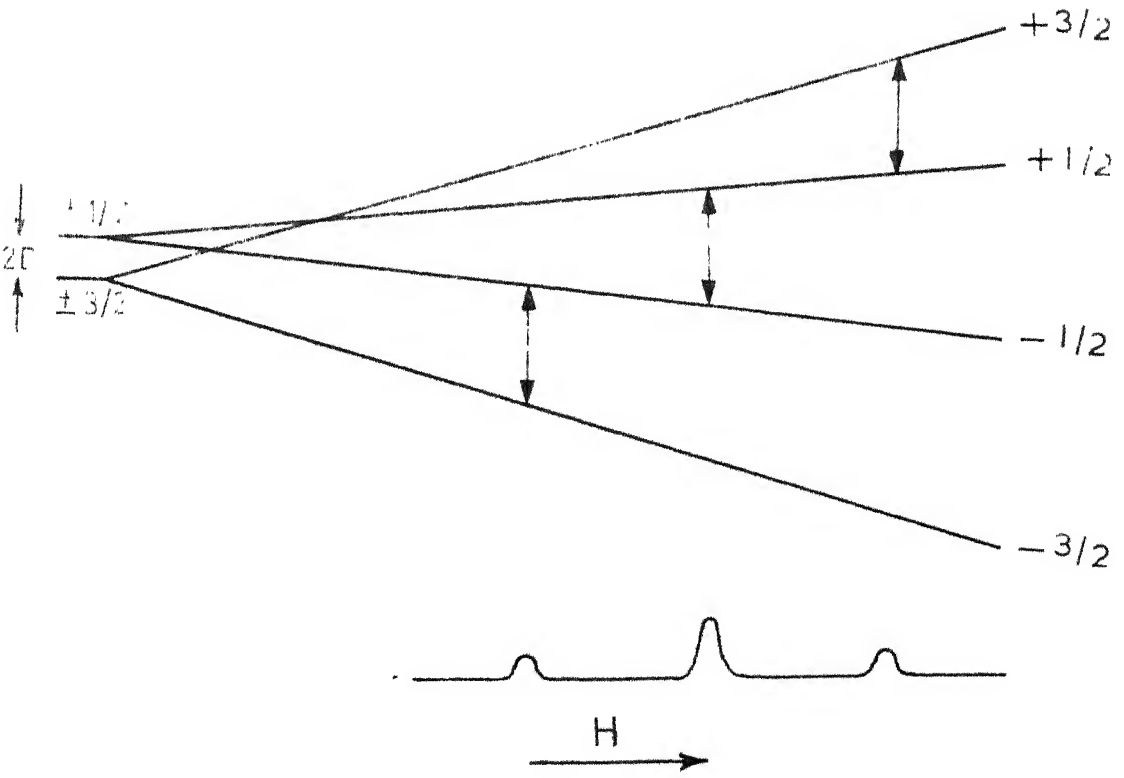

II . II-1 $\Delta M = \pm 1$ transitions for the two cases of complete and partial degeneracies, in the absence of the Zeeman field, for J = 3/2. 2D is the initial separation between the $\pm$ 3/2 and $\pm$ 1/2 levels.

since these preserve their unfilled electronic shells in their ionic states. In solids the paramagnetic ions are surrounded by various atoms and molecules. The spectroscopic properties of paramagnetic ions in solids are well explained by regarding the surrounding atoms and molecules as point charges or dipoles fixed at appropriate lattice points.[1,2] These point charges or dipoles are termed as ligands. These ligands produce an electrostatic field (also called as ligand field or crystalline field) of appropriate symmetry and strength at the paramagnetic ion. The energy levels of the paramagnetic ion are split depending upon the symmetry and strength of the crystalline field.

Now we shall consider the Hamiltonian of a paramagnetic ion and the effect of the crystalline field, denoted by $\mathcal{H}_{cr}$.

The Hamiltonian of a paramagnetic ion without the crystalline field and Zeeman-field interactions is written as

$$\mathcal{H} = \mathcal{H}_F + \mathcal{H}_{LS} + \mathcal{H}_{SS} + \mathcal{H}_N. \qquad \text{(II.4)}$$

$\mathcal{H}_F$ is the free-ion Hamiltonian, given by

$$\mathcal{H}_F = \sum_{k=1}^{N} (P_k^2/2m - Ze^2/r_k) + \sum_{k<j=1}^{N} (e^2/r_{jk}), \qquad \text{(II.5)}$$

where N is the number of outer electrons. $\mathcal{H}_{LS}$ is the magnetic interaction between the electron spins $\vec{s}_k$ and the orbital angular momenta $\vec{l}_k$, and is given by

$$\mathcal{H}_{LS} = \sum_{j,k} (a_{jk}\vec{l}_j \cdot \vec{s}_k + b_{jk}\vec{l}_j \cdot \vec{l}_k + c_{jk}\vec{s}_j \cdot \vec{s}_k). \qquad \text{(II.6)}$$

The spin-spin interaction term[3] is given by

$$\mathcal{H}_{SS} = \sum_{j,k} \frac{1}{r_{jk}^3}[\vec{s}_j \cdot \vec{s}_k - 3(\hat{r}_{jk} \cdot \vec{s}_j)(\hat{r}_{jk} \cdot \vec{s}_k)], \quad \text{(II.7)}$$

where $\hat{r}_{jk}$ is a unit vector along $\vec{r}_{jk}$. The hyperfine interaction consists of two terms, the dipolar term

$$\mathcal{H}_{dN} = 2\gamma\beta\beta_N \sum_k \frac{1}{r_k^3}[(\vec{l}_k - \vec{s}_k) \cdot \vec{I} + 3(\vec{r}_k \cdot \vec{s}_k)(\vec{r}_k \cdot \vec{I})], \quad \text{(II.8)}$$

and the contact term due to the s-state electrons

$$\mathcal{H}_{cN} = 2\gamma\beta\beta_N \sum_k (8\pi/3)\delta(\vec{r}_k)(\vec{s}_k \cdot \vec{I}), \quad \text{(II.9)}$$

where γ is the nuclear gyromagnetic ratio, β_N the nuclear magneton, and $\vec{I}$ the nuclear spin. In addition, the electrostatic interaction with the quadrupole moment Q of the nucleus gives

$$\mathcal{H}_Q = [e^2Q/2I(I-1)] \sum_k \frac{1}{r_k^3}[I(I+1) - 3(\vec{r}_k \cdot \vec{I})]. \quad \text{(II.10)}$$

All these three add to form $\mathcal{H}_N$, i.e.

$$\mathcal{H}_N = \mathcal{H}_{dN} + \mathcal{H}_{cN} + \mathcal{H}_Q. \quad \text{(II.11)}$$

The orders of magnitudes of these interactions are,[4] $\mathcal{H}_F \sim 10^5$ cm^{-1}, $\mathcal{H}_{LS} \sim 10^2$ cm^{-1} for the iron group ions, $\mathcal{H}_{SS} \sim 1$ cm^{-1}, and $\mathcal{H}_N \sim 10^{-2}$ cm^{-1}. Now we consider the effect of the crystalline field.

For the case of iron group ions, with which we are presently concerned, Russell - Saunders coupling is a good approximation and one can write

$$\mathcal{H}_{LS} = \lambda \vec{L}\cdot\vec{S},$$

$$\mathcal{H}_{SS} = \rho\left[\tfrac{1}{2}(L_iL_j + L_jL_i)S_iS_j - \tfrac{1}{3}L(L+1)S(S+1)\right],$$

$$\mathcal{H}_{dN} = (2\gamma\beta\beta_N/r^3)\left[(\vec{L}\cdot\vec{I}) + \xi L(L+1)(\vec{S}\cdot\vec{I}) - \tfrac{3}{2}\xi(\vec{L}\cdot\vec{S})(\vec{L}\cdot\vec{I}) - \tfrac{3}{2}\xi(\vec{L}\cdot\vec{I})(\vec{L}\cdot\vec{S})\right],$$

$$\mathcal{H}_{cN} = (-2\gamma\beta\beta_N k/r^3)(\vec{S}\cdot\vec{I}),$$

and,

$$\mathcal{H}_Q = [\eta e^2Q/2I(2I-1)r^3]\left[3(\vec{L}\cdot\vec{I})^2 + \tfrac{3}{2}(\vec{L}\cdot\vec{I}) - L(L+1)I(I+1)\right]. \quad \ldots \quad (II.12)$$

λ is called the spin-orbit constant and ρ, ξ, and η are other constants. Depending on its magnitude relative to other terms in $\mathcal{H}$, the crystalline field interaction $\mathcal{H}_{cr}$ is classified into three classes.

(a) Weak field: This is the case when the crystalline field interaction is weaker than the spin-orbit interaction. This situation exists in ions of rare earth group, where the magnetic 4f electrons are shielded from the crystalline field, by the outer $5s^2 5p^6$ electrons.

(b) Medium field: The effect of the crystalline field is greater than the spin-orbit interaction, but is less than the mutual interaction between electrons. The best examples of these are the hydrated salts of the iron group.

(c) Strong field: The crystalline field is of the order of the energy of mutual interaction between electrons. This occurs

notably in the cyanides of the iron group and the Palladium (4d) and Platinum (5d) group.

The magnitude of $\mathcal{H}_{cr}$ relative to other terms in $\mathcal{H}$ decides the spectroscopic and magnetic properties of ions of transition group elements. It has been observed that in the case of iron group ions, the experimentally measured susceptibility agrees well with the spin only contribution. This means that in this group, the orbital angular momentum is largely quenched.[5] For iron group ions $\mathcal{H}_{cr} \sim 10^4$ cm^{-1}.[4]

When the Zeeman field $\vec{H}$ acts on the system, the interaction is given by

$$\mathcal{H}_Z = \hbar\beta(\vec{L}+2.0023\vec{S})\cdot\vec{H}. \qquad \text{(II.13)}$$

Here we have neglected the direct interaction of $\vec{H}$ with the nuclear magnetic moment. For typical fields of $\vec{H}$ obtainable in the laboratory $\mathcal{H}_Z \sim 1$ cm^{-1}. Thus the total Hamiltonian, including all the interactions, is written as

$$\mathcal{H}_{Tot} = \mathcal{H}_F + \mathcal{H}_{cr} + \mathcal{H}_{LS} + \mathcal{H}_Z + \mathcal{H}_{SS} + \mathcal{H}_N. \qquad \text{(II.14)}$$

Spin-Hamiltonian Formalism:

In EPR one is concerned only with the ground state manifold of energy levels of an ion, lying within few cm^{-1}. Hence it is more convenient, in the case of iron group ions, to solve the total Hamiltonian $\mathcal{H}_{Tot}$ in the ground manifold of $\mathcal{H}_F + \mathcal{H}_{cr}$ and consider the other terms as perturbations

over this manifold. This method of solving the Hamiltonian, to evaluate the energy levels of interest in EPR, has been due to Pryce,[6] and Abragam and Pryce.[4]

Two cases arise here, the ions whose ground state manifold in the presence of the crystalline field is orbitally degenerate, and those whose ground state is orbitally non-degenerate. As we are concerned only with those ions (Mn^{2+}) whose ground state is orbitally non-degenerate, we have

$$\langle 0|\vec{L}|0\rangle = 0,$$

$$\frac{1}{2}\langle 0|L_iL_j+L_jL_i|0\rangle = \frac{1}{3}L(L+1)\delta_{ij} + l_{ij}, \quad (l_{ii} = 0). \qquad \ldots(II.15)$$

Also we define

$$\Lambda_{ij} = \sum_{n\neq 0} \frac{\langle 0|L_i|n\rangle\langle n|L_j|0\rangle}{E_n-E_o}, \quad i,j = 1,2,3,$$

and

$$u_{ij} = \frac{i}{2}\epsilon_{ikl} \sum_{n\neq 0} \frac{\langle 0|L_i|n\rangle\langle n|L_jL_k+L_kL_j|0\rangle}{E_n-E_o},$$

$$u_{ii} = 0, \quad i,k,l = 1,2,3. \qquad \ldots(II.16)$$

The order of perturbation to be carried out is limited by its contribution to the energy level evaluation. For the case where the ground state is orbitally non-degenerate, the second order contribution from $\mathcal{H}_{LS}$ is comparable to the first order contribution of $\mathcal{H}_Z$, and hence the perturbation is carried out to the second order. Higher order terms are much small. Thus the new Hamiltonian, where only terms upto

the second order have been included, i.e.,

$$\mathcal{H}_S = 2.0023\beta(\delta_{ij}-\lambda\Lambda_{ij})H_iS_j + (-\lambda^2\Lambda_{ij}-\sigma_{ij})S_iS_j - P(k\delta_{ij}+3\kappa_{ij}+2\lambda\Lambda_{ij}-3\kappa_{ij})S_iI_j + q'\Lambda_{ij}I_iI_j. \quad (II.17)$$

This can be written in an abbreviated form as

$$\mathcal{H}_S = \beta g_{ij}H_iS_j + D_{ij}S_iS_j + A_{ij}S_iI_j + Q_{ij}I_iI_j. \quad (II.18)$$

This Hamiltonian is called the 'spin Hamiltonian'. The greatest advantage of the spin Hamiltonian is the simplicity of its form, where the various interactions acting on the ion have been reduced to a relatively few spin-Hamiltonian constants. This spin S is called the 'effective' or 'fictitious' spin, as this may not be the actual spin of the electronic system. When the ground state of the ion in the manifold $\mathcal{H}_F + \mathcal{H}_{cr}$ is an orbital singlet, the actual and effective spins are one and the same. The effective spin is an experimentally determined quantity and is obtained by equating the number of magnetic dipole transitions to 2S.

As can be seen, g_{ij}, D_{ij}, A_{ij}, and Q_{ij} are all second rank tensors, The system of orthogonal axes, where these tensors are completely diagonal (i = j), is known as the principal-axes system. The principal axes are determined by the crystalline field acting at a particular paramagnetic ion. Hence these are different, for ions with different crystalline environments, and even for ions with the same environment when they are differently oriented (as is sometimes the

case when the number of molecules in unit cell of a single crystal is more than one). The orthogonal sets of principal axes for a particular paramagnetic ion, and the susceptibility axes for the unit cell, are not related to each other unless either there is only one paramagnetic ion per unit cell or all the paramagnetic ions in the unit cell are magnetically equivalent - i.e. when all the sets of principal axes are either parallel or antiparallel. The magnitudes of g_{ij}, D_{ij}, etc. in the principal axes system are called the spin-Hamiltonian constants or parameters, and these are evaluated from the EPR experiments. The usage of the same subscript twice (like g_{xx}, etc.), is replaced by a single subscript (g_x, etc.,). Instead of D_x, D_y, and D_z, one defines $D = (3/2)D_z$ and $E = (1/2)(D_x - D_y)$, and similarly $Q' = (3/2)Q_z$ and $Q'' = (1/2)(Q_x - Q_y)$. Thus, in the principal axes system, the spin Hamiltonian, Eq.(II.18) is written as,

$$\mathcal{H}_S = \beta g_z H_z S_z + \beta g_x H_x S_x + \beta g_y H_y S_y + D[S_z^2 - S(S+1)/3] + E(S_x^2 - S_y^2) + A_z S_z I_z + A_x S_x I_x + A_y S_y I_y + Q'[I_z^2 - I(I+1)/3] + Q''(I_x^2 - I_y^2). \qquad (II.19)$$

Hereafter the word spin means the effective spin, and axes, the principal axes.

It is the preferred choice of the axes for each ion, the extreme sensitivity of the spin-Hamiltonian parameters to the symmetry and strength of the crystalline field, and

the wide usage of magnetically dilute crystals, that has made the study of EPR in single crystals more information-rendering. We now consider the spin-Hamiltonian parameters individually.

(a) g factor: The Lande g factor for an ion with an orbital angular momentum $\vec{L}$, spin angular momentum $\vec{S}$, and a total angular momentum $\vec{J}$ is given by

$$g_{\text{Lande}} = 1 + \frac{J(J+1) + S(S+1) - L(L+1)}{2J(J+1)} . \qquad \text{(II.20)}$$

But it has been found that for most of the iron group ions in solids, the contribution to the experimentally obtained magnetic susceptibility came mostly from spin only angular momentum. Thus for the paramagnetic ions in solids, a new g value, which obeys Eq. (II.1), is defined. This g value is purely an experimentally determined parameter and is called the spectroscopic splitting factor. Also it is seen from Eq. (II.19) that g is a second rank tensor, its symmetry being the symmetry of the crystalline field (e.g. for an axial crystalline field, $g_z \neq g_x = g_y$). Even for ions whose ground state manifold in the crystalline field is an orbital singlet, g is not equal to 2.0023, but differs by an amount depending on the magnitude of λ and Λ_{ij}.

(b) D and E: In the absence of the Zeeman interaction and the hyperfine interactions, D and E are a measure of the energy separations within the spin multiplet, indicating that

the degeneracy in the absence of the Zeeman field is not 2S+1. This leads to the 'fine structure'. D and E are called the fine-structure constants. D represents axial part and E the rhombic part of the crystalline field.

(c) A_x, A_y, A_z, Q' and Q'': A symmetric state like that of Mn^{2+} is not expected to show hyperfine structure, but Mn^{2+}, as also other paramagnetic ions with non-zero nuclear spin, exhibits predominant hyperfine structure. This necessitated the idea of configuration mixing[7] of the $3d^5$ state with $3d^4 4s$ state. The detailed estimation of the hyperfine structure interaction was done by Abragam et al.[6,8] If the Zeeman field is strong enough to break the coupling between the electronic and nuclear moments, the hyperfine structure shows up without affecting the positions of the fine-structure transitions. Because of the selection rule for hyperfine transitions ($\Delta m=0$, $m=I_z$), the nuclear spin is readily obtained by equating the number of hyperfine transitions to 2I+1. The second order shift in the hyperfine separations, or the appearance of $\Delta m = \pm 1$ transitions, facilitates the computation of Q' and Q''.

Allowed and Forbidden Transitions:

When the oscillating field is kept perpendicular to the Zeeman field, the allowed electronic transitions are the magnetic dipole ($\Delta M = \pm 1$, $M = S_z$, S_x, or S_y) transitions. As the microwave field exerts a negligible effect on the nuclear

moments, the selection rule involving nuclear transitions is $\Delta m = 0$. The transitions ($\Delta M = \pm 1$, $\Delta m = 0$) are called the allowed transitions. In addition, transitions other than the allowed ones are sometimes observed when the Zeeman-field direction is off the axes. Transitions where $\Delta M \neq 1$ are called electronic forbidden transitions. These occur due to the mixing of the states with (M-2) and other quantum numbers with the (M-1) state, due to the non-diagonal terms involving $S_z S_{\pm}$ etc.[9,10] The $\Delta M = \pm 2$ transitions occur at Zeeman-field intensities about half the magnitude for ($\Delta M = \pm 1$) transitions. Transitions involving $\Delta m \neq 0$ are called hyperfine or nuclear forbidden transitions. These occur because of the second order mixing of the hyperfine constant A with the fine structure constant.[11] $\Delta m = \pm 1$ transitions result in the appearance of doublets (corresponding to $\Delta m = +1$ and $\Delta m = -1$) in between the allowed transitions corresponding to $M = +1/2 \leftrightarrows -1/2$ transition.

Fine Structure of Mn^{2+}:

Divalent manganese has a ground state configuration of $(3d)^5$ electrons and hence the ground state $^6S_{5/2}$. When placed in a crystalline field this orbitally non-degenerate ground state splits into a doublet and a quartet in cubic field, and into three doublets (Kramers doublets) in low symmetry fields.[12] This gives rise to the fine structure in the EPR of Mn^{2+}. The theoretical prediction of the magnitude and

sign of the fine-structure splitting (D and E) has been of considerable interest since the very early days[13] when these splittings were observed in the susceptibility experiments. The various mechanisms have been,

(a) the spin-spin interaction and the admixture of the state $3d^4 4s$ due to Pryce,[3]

(b) the spin-spin and the spin-orbit interactions between the states from within the $3d^5$ configuration by Watanabe,[14]

(c) the spin-orbit admixture with the excited $^4\Gamma_4$ level (in a cubic field) due to Blume and Orbach,[15] and

(d) the configurational admixing by adding the axial field potential to the Hartree-Fock potential to obtain s-, t-, and g- like admixtures due to Orbach et al.[16] The magnitude of these mechanisms were considered by Sharma et al.[17] using the point charge model and also considering the overlap and charge transfer effects. The variation of cubic field splitting of Mn^{2+} in MgO was fit by assuming the cubic field splitting mechanism to be due to the phonon-induced crystal-field effects by Shrivastava.[18] In addition, Wybourne[19] has shown that relativistic effects can produce second order crystal-field splitting of the S-state ions. This method was applied to the case of Mn^{2+} by Heuvelen.[20]

In general, the experimental splittings have been found to be due to the combined effect of all these, although of varying magnitudes. The various interactions, and the allowed transitions in the EPR of Mn^{2+}, are shown in Fig. II-2.

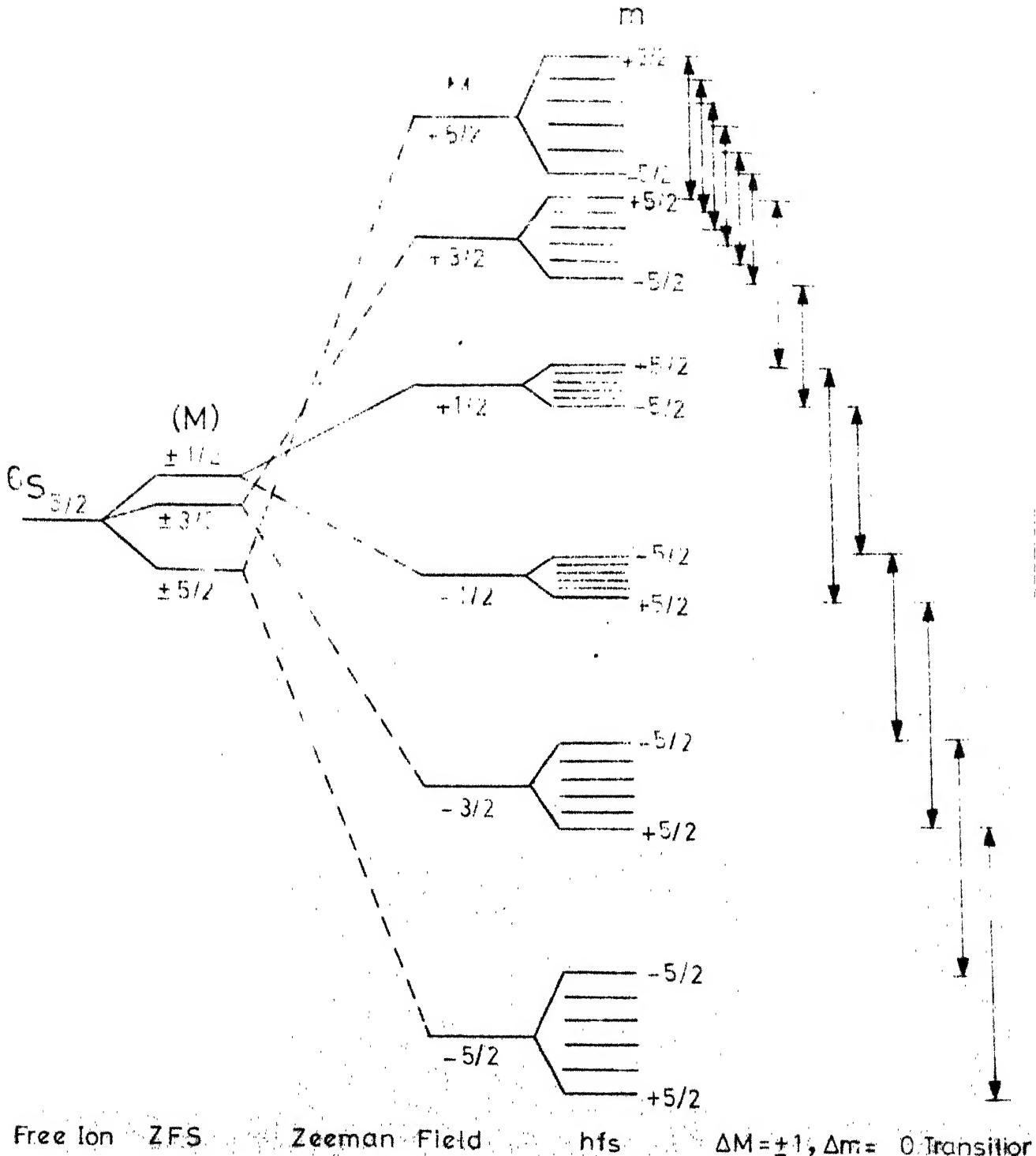

Fig. II-2: Energy level splittings of the ground state of Mn^{2+}, for the case of negative D, and the $\Delta M = \pm 1$, $\Delta m = 0$ transitions. ZFS is the spl ing due to the crystalline field, and hfs due to the hyperfine interact

Kramers Theorem:

This theorem states that a purely electrostatic field acting on a system of odd number of electrons can not reduce its degeneracy below two. This is due to the invariance property of the system under time reversal.[12] A natural and welcome consequence of Kramers theorem is that EPR can always be observed in systems with odd numbers of elections. The examples are Cr^{3+}, Mn^{2+}, Co^{2+}, etc.

Jahn - Teller Effect:

Unlike Kramers degeneracy, which retains a minimum degeneracy, Jahn-Teller effect removes the degeneracy. This effect[21] states that if the electronic state of a system is degenerate, the geometric configuration of its nuclei can not be stable (except in linear molecules and Kramers systems) and hence by a lowering of the symmetry of nuclear configuration the degeneracy of the electronic state is lifted. The examples are Cu^{2+} in trigonal symmetry, Co^{2+} and Fe^{2+} in cubic (octahedral) fields.

Spin-Spin and Spin-Lattice Interactions:

The paramagnetic ions (spins) in a medium (lattice) interact among themselves and with the medium. These interactions cause broadening of the absorption lines. When one is interested in the study of the details of the interactions - like the crystalline field and hyperfine splitting, the

contributions to the linewidth due to the spin-spin and spin-lattice interactions is reduced. The spin-spin interactions are minimized by using magnetically dilute crystals, and the spin-lattice interactions by working at low temperatures.

The spin-spin interaction acts in two ways viz., the magnetic dipolar and the electrostatic exchange interactions. The dipolar interaction can be considered as the interaction between two magnetic dipoles, which sets up local magnetic fields in addition to the Zeeman field. This results in a broadening of the absorption lines. The exchange interactions were introduced when purely dipolar interactions could not account for the observed linewidths - like the narrowing of resonance lines in the case of like spins, with decrease in their distance. But the exchange interactions between non-identical spins cause broadening of the absorption lines. Unlike the dipolar interactions, exchange interactions are very short range interactions. The spin-spin interactions are very little dependent on the temperature and can be reduced by increasing the separation between the spins, i.e. by diluting in a diamagnetic lattice.

The spin-lattice interaction decides how fast the spin returns to thermodynamical equilibrium, by exchange of its energy to the lattice, after the equilibrium has been disturbed by the absorption of microwave energy. This exchange of energy takes place in two ways.

(a) Direct Process: The spin transfers the energy absorbed ($h\nu$) to the lattice with a corresponding creation of a phonon of energy $h\nu$. This process is proportional to the temperature, T of the lattice.

(b) Indirect Process: In this mechanism a high frequency phonon of energy $h\nu'$ is inelastically scattered by the spin which results in the creation of a phonon $h\nu'' = h\nu + h\nu'$. As in this process many modes of lattice vibrations of high frequency are put into action, it is predominant only at higher temperatures. This process is proportional to T^7 of the lattice.

In addition to these, in some cases where the splittings in crystalline fields are smaller than the energy of the phonons, as is the case in some rare earth ions, relaxation via an intermediate state of Zeeman levels takes place. This is known as the Orbach process.

The spin-lattice interaction is very much temperature-dependent and is reduced by working at low temperatures. It has also been observed that the spin-lattice interactions is dependent on the separation of the first excited state of the spin over its ground state.[22] For S-state ions, like Mn^{2+}, the spin-lattice interactions are not predominant so that the EPR of these ions can be observed at room temperature.

EPR of Mn^{2+} in Paramagnetic Single Crystals:

In the present study we are interested in the effect, on the EPR of Mn^{2+}, due to the paramagnetic cations of single crystals, which do not exhibit their EPR at room temperature and at X-band microwave frequency due to the following reasons.

(a) The paramagnetic cations have very short spin-lattice relaxation time at the studied temperatures, so that their absorption lines become too weak and too broad to be observed,[23] like Fe^{2+} in $Fe(NH_4)_2(SO_4)_2 \cdot 6H_2O$.

(b) The orbital and spin degeneracies of the paramagnetic cations are completely removed in the presence of the crystalline field of lower-than-axial symmetry. This can happen to ions having even number of outer electrons. For these cases, the ground state is a spin and orbital singlet and hence does not possess any magnetic moment. But interactions with the excited states introduce magnetic moments which are observed when the Zeeman field is applied. This is obtained as follows:

The energy of the system, in the presence of the Zeeman-field H, is written as[25]

$$E = W_o + W_1 H + W_2 H^2 + \ldots . \qquad (II.21)$$

The magnetic moment then is given by

$$M = \text{constant} \times \frac{\partial E}{\partial H}$$

$$= \text{constant} \left[W_1 + 2W_2 H + \ldots . \right]. \qquad (II.22)$$

Here

$$W_1 = \langle \bar{0} | \beta(L_{II} + 2S_{II}) | 0 \rangle, \qquad \text{(II.23)}$$

$$W_2 = \sum_{n \neq 0} |\langle \bar{n} | \beta(L_{II} + 2S_{II}) | 0 \rangle|^2 / (E_n - E_0), \qquad \text{(II.24)}$$

and etc.

For these systems $W_1 = 0$, but W_2, etc. contribute to the magnetic moment when the Zeeman field is applied. The examples of such ions are Ni^{2+} ions in lower-than-axial symmetry crystalline fields. The effect of these ions on the EPR of Mn^{2+}, and other ions has been considered in detail by Moriya and Obata,[26] and Hutchings and Wolf.[27]

REFERENCES

1. W.G. Penney and R. Schlapp, Phys. Rev. 41, 194 (1932).
2. R. Schlapp and W.G. Penney, ibid. 42, 666 (1932).
3. M.H.L. Pryce, ibid. 80, 1107 (1950)..
4. A. Abragam and M.H.L. Pryce, Proc. Roy. Soc. (London) A205, 135 (1951).
5. J.H. Van Vleck, 'The Theory of Electric and Magnetic Susceptibilities', The University Press, Oxford (1965).
6. M.H.L. Pryce, Proc. phys. Soc. (London) A63, 25 (1950).
7. A. Abragam, Phys. Rev. 79, 534 (1950).
8. A. Abragam, J. Horowitz, and M.H.L. Pryce, Proc. Roy. Soc. (London) A230, 169 (1955).
9. B. Bleaney and D.J.E. Ingram, ibid. A205, 336 (1951).
10. C. Marti, R. Romestain, and R. Vasockas, Phys. Status Solidi 28, 97 (1968).
11. B. Bleaney and R.S. Rubins, Proc. phys. Soc. (London) 77, 103 (1961) and 78, 778 (1961).
12. W. Low, 'Paramagnetic Resonance in Solids', Academic Press, New York (1960).
13. J.H. Van Vleck and W.G. Penney, Phil. Mag. 17, 961 (1934).
14. H. Watanabe, Prog. theor. Phys. 18, 405 (1957).
15. M. Blume and R. Orbach, Phys. Rev. 127, 1587 (1962).
16. R. Orbach, T.P. Das, and R.R. Sharma, Proc. int. Conf. on Magnetism, Nottingham (1964).
17. R.R. Sharma, T.P. Das, and R.Orbach, Phys. Rev. 149, 257 (1966) and 155, 338 (1967).
18. K.N. Shrivastava, ibid. 187, 446 (1969).

19. [illegible] Wyderman, J. Chem. Phys. 43, 4506 (1965).

20. A.V. [illegible], [illegible]. 46, 4903 (1967).

21. S.A. Al'tshuler and B.M. Kozyrev, 'Electron Paramagnetic Resonance', Academic Press, New York (1960).

22. B. Bleaney and K.W.H. Stevens, in 'Reports on Progress in Physics' (Ed. A.C. Stickland) Vol. 16, p.108. Published by the Physical Society, London (1953).

23. B. Bleaney, R.J. Elliott, and H.E.D. Scovil, Proc. Phys. Soc. (London) A64, 933 (1951).

24. J. H. Griffiths, 'The Theory of Transition Metal Ions', The University Press, Cambridge (1961).

25. T. Moriya and Y. Obata, J. phys. Soc. Japan 13, 1333 (1958).

26. D.T. Hutchings and W.P. Wolf, Phys. Rev. Lett. 11, 187 (1963).

GENERAL REFERENCES

1. B. Bleaney and K.W.H. Stevens, in 'Reports on Progress in Physics' (Ed. A.C. Stickland) Vol. 16, p. 108. Published by the Physical Society, London (1953).

2. K.D. Bowers and J. Owen, ibid. Vol. 18, p. 304. (1955).

3. W. Low, 'Paramagnetic Resonance in Solids', Academic Press, New York (1960).

4. S.A. Al'tshuler and B.M. Kozyrev, 'Electron Paramagnetic Resonance', Academic Press, New York (1960).

5. G.E. Pake, 'Paramagnetic Resonance', Benjamin, New York (1962).

CHAPTER III

EXPERIMENTAL DETAILS

Abstract

A brief description, of the experimental setup, the crystal rotator used to rotate the crystal spatially inside the cavity, the simultaneous equations used for the analysis of the observed spectra, and the regression theory used to fit the experimental data of linewidth variation of the resonance lines with the intensity of the Zeeman field, is given.

EPR Spectrometer:

The experiments were conducted on a Varian V-4502 EPR spectrometer[1] operating at the X-band microwave frequency region (~ 9.5 GHz). A block diagram of the spectrometer is given in Fig. III-1. The Zeeman field at the site of the crystal inside the cavity was modulated by 100 kHz frequency modulation. The microwave output from the klystron of fixed frequency is locked to the cavity resonating frequency by means of an automatic frequency control (AFC) using a reference frequency of 10 kHz. This microwave output, after being attenuated to the proper power, is divided between the two arms of a hybrid tee, one of which has the reflection cavity at its end. The crystal detector is in the fourth arm on which microwaves are incident only when there is imbalance in the reflected power in arms 2 and 3, due to the absorption of microwave power by the sample placed in the cavity. The 100 kHz modulated microwave power output, which contains the EPR signal, is detected by means of a phase sensitive detector and recorded on a Varian G-14 strip chart recorder. The Zeeman field between the 9" magnet pole pieces is varied linearly from near zero to about 10 kilogauss, by means of a driving mechanism, which changes linearly with time the control voltage applied to the input of the current regulated magnet power supply. Two kinds of reflection cavities were used,

(a) the cylindrical cavity (Varian V-4533) operating in the

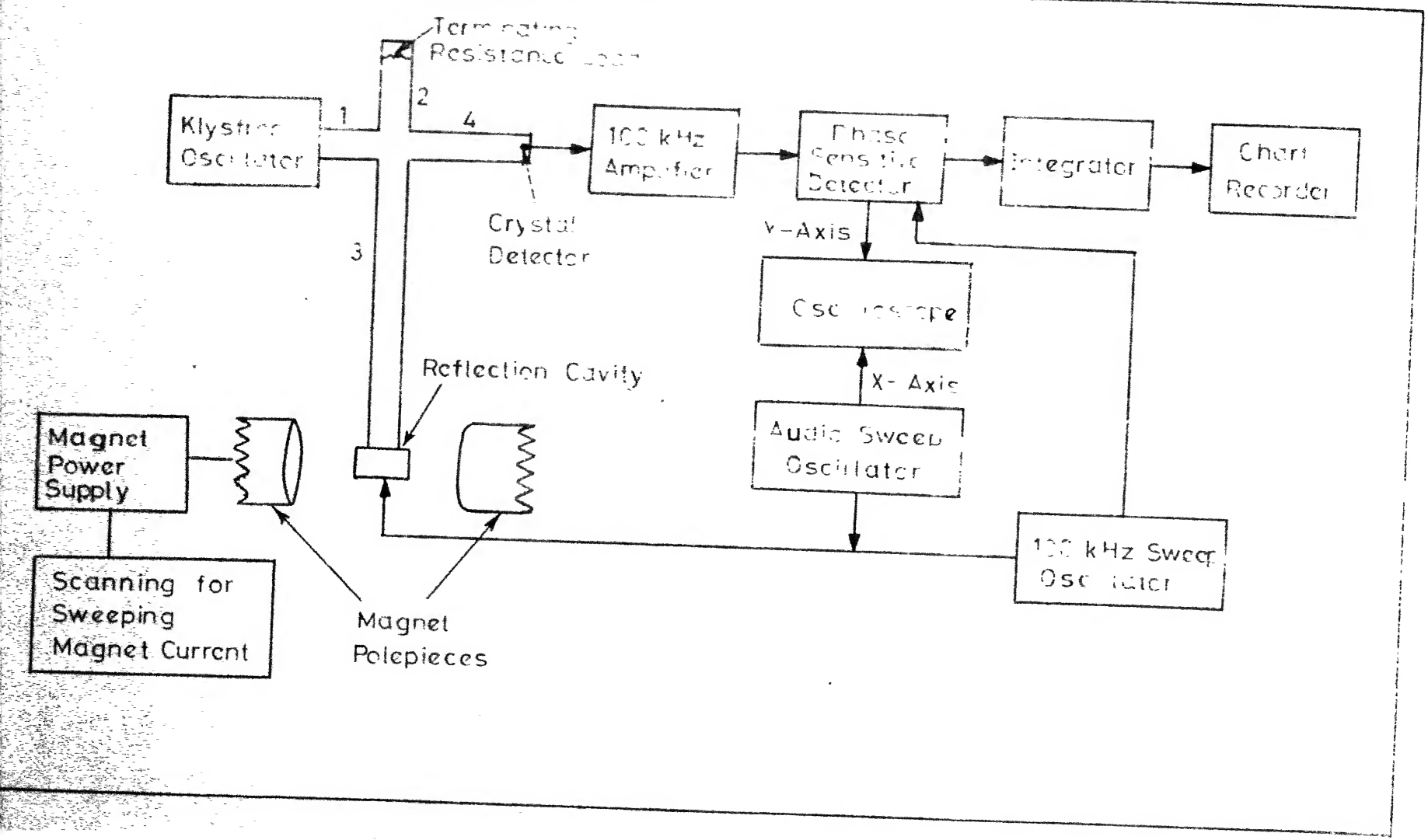

Fig. III-1: Block diagram of the EPR spectrometer.

TE_{011} mode for variation of the Zeeman-field direction relative to the crystalline axes, and

(b) the multipurpose rectangular cavity (Varian V-4521) operating in the TE_{102} mode for temperature variation.

Crystal Rotator:

The angle between the Zeeman-field direction and the crystalline axes can be varied by rotating the magnet about the vertical axis. In addition, to provide a spatial orientation, the crystal was mounted on a crystal rotator so as to be rotated about a horizontal axis. Thus it has become possible by rotating the crystal within the cavity about a horizontal axis and the Zeeman field about the vertical axis, to align any desired axis of the crystal with the Zeeman-field, without removing the crystal whenever the orientation has to be changed. The rotation of the crystal about a horizontal axis has been achieved by means of a thread and shaft arrangement. The crystal rotator is shown in Fig. III-2. Whenever the orientation of the crystal in the cavity was changed, the klystron was tuned to the cavity resonating frequency.

Crystal Growth:

The single crystals of all the compounds in the present study were grown by slow evaporation of a saturated solution, of the particular compound and about 2 percent of the corresponding manganese compound by weight, in distilled water at

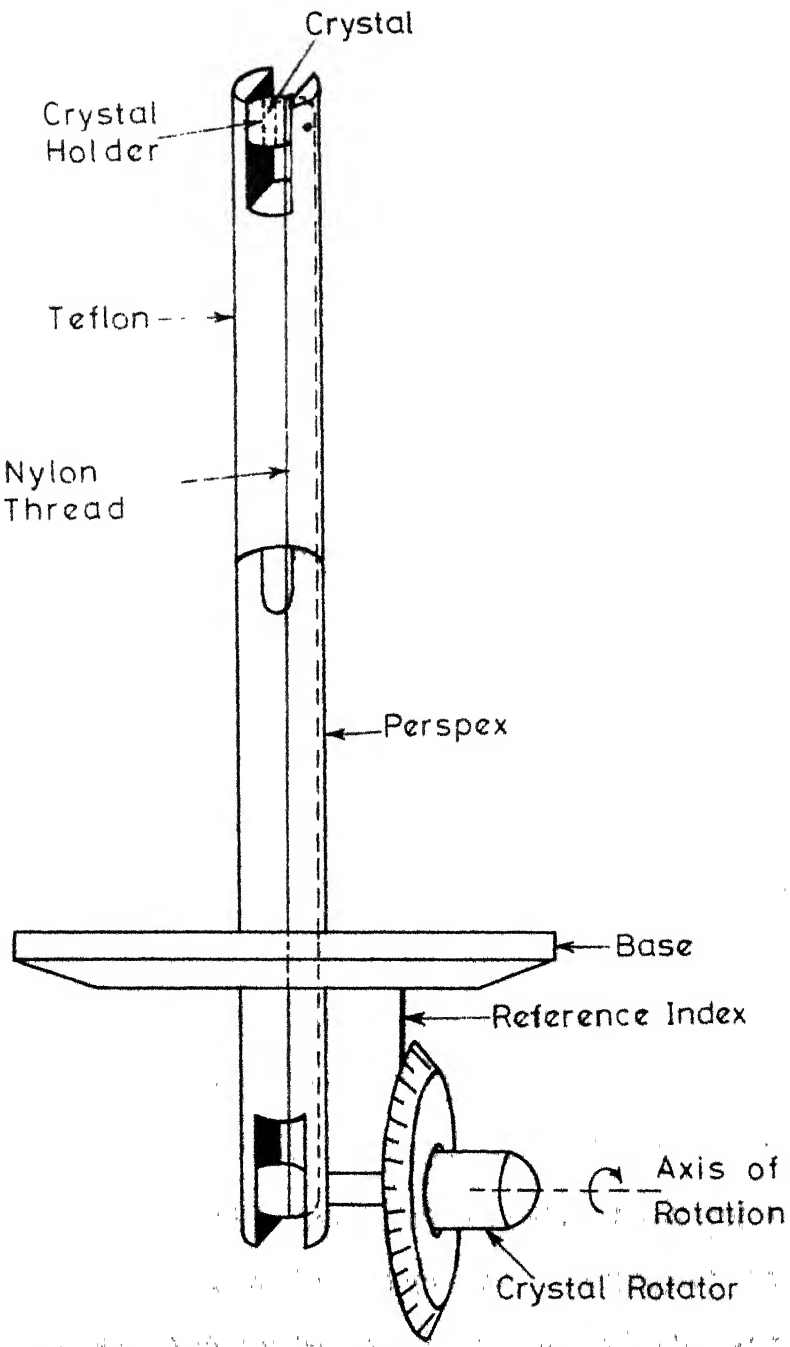

Fig. III-2 Device to rotate the single crystal inside the cavity about a horizontal axis.

constant temperature. $Ni(CH_3COO)_2 \cdot 4H_2O$ was prepared in the laboratory, while other compounds of the required purity were purchased. The crystals of Mn^{2+}-doped $NiSO_4 \cdot 7H_2O$ were grown from an initial compound of $NiSO_4 \cdot 6H_2O$ using the method given by Holden and Singer.[2] The single crystals were coated with a thin layer of petroleum jelly and paraffin oil mixed in the ratio 1:1 by volume, to protect them from exposure to atmosphere.

Analysis of the Spectra:

The observed spectra of Mn^{2+} ($S = 5/2$, $I = 5/2$), corresponding to $\Delta M = \pm 1$, $\Delta m = 0$ transitions, have been analyzed for the spin-Hamiltonian constants by fitting the resonance field values to the transitions between the appropriate energy levels given by the spin Hamiltonian, Eq. (II.19) .Where there were more than one magnetically equivalent complexes, the transitions along the z axis were identified by the angular variation of the spectrum near the z axis.[3] This is because the transitions corresponding to the Zeeman field parallel to the z axis move less rapidly than the others. The relative signs of the spin-Hamiltonian constants, assuming the hyperfine constant A to be of negative sign, were assigned by the second order shift in the hyperfine separations of the various fine-structure transitions.[3] Depending on the magnitude of D and E relative to the Zeeman term and the magnitude of E relative to D, the order of perturbation necessary to evaluate the

spin-Hamiltonian constants is limited. For D and E << Zeeman-term, and E < D, terms upto third order as given by Chambers et al.[4] were found to be sufficient, for our systems. These equations, in the units of Zeeman field, and for the Zeeman field along the z axis, are given here.

a) Fine-structure transitions:

$$H(M = \pm\tfrac{5}{2} \leftrightarrows \pm\tfrac{3}{2}) = H_o \mp 4D + 4(E^2/H_o) \pm 6(DE^2/H_o^2) + 36(D^2E^2/H_o^3) + 28(E^4/H_o^3),$$

$$H(M = \pm\tfrac{3}{2} \leftrightarrows \pm\tfrac{1}{2}) = H_o \mp 2D - 5(E^2/H_o) \pm 33(DE^2/H_o^2) + 45(D^2E^2/H_o^3) - (5/4)(E^4/H_o^3),$$

and $$H(M = \pm\tfrac{1}{2} \leftrightarrows \mp\tfrac{1}{2}) = H_o - 8(E^2/H_o) + 72(D^2E^2/H_o^3) + 56(E^4/H_o^3).$$

... (III.1)

(b) Hyperfine separations:

$$H(m \leftrightarrows m) = -Am - \frac{B^2}{2H_o}\left[\frac{35}{4} - m^2 + m(2M-1)\right]. \qquad \text{(III.2)}$$

When the Zeeman field is along x or y axis the spin Hamiltonian, Eq.(II.19), and accordingly the above equations, are modified by replacing D by (1/2)(3E-D) and E by (-1/2)(D+E) for H along x axis, and for H along y D is replaced by (-1/2)(D+3E) and E by (1/2)(D-E).[5]

The resonance field intensities for each transition were obtained by finding the resonance field value of the standard organic radical, diphenyl picryl hydrazil (DPPH).

The resonance Zeeman-field intensity for DPPH was obtained by measuring the proton resonance frequency at that field. The g value for a particular complex was calculated by comparison with DPPH, g = 2.0036.

Method of Linear Regression:

In Chapters VI and VII we present the results of the variation of linewidth (Δ H) of the Mn^{2+} resonance lines with the intensity (H) of Zeeman field. The best fit between these two parameters was done by the linear regression method.[6] A very brief introduction to the method of fitting by the linear regression method is given here.

This method states that if there are two simultaneously observed variables x and y, and if the two can be related by a linear equation of the form

$$y = a + bx, \qquad \text{(III.3)}$$

where x is selected by the experimenter (H or H^2), and y is the corresponding values at x (ΔH), the standard method of estimation in regression is to use those values of a and b which will minimize the sum of squares of deviation (say R), between the observed y_i and the estimated Y_i. R is given by

$$\begin{aligned} R &= \Sigma(y_i - Y_i)^2 \\ &= \Sigma(y_i - a - bx_i)^2, \end{aligned} \qquad \text{(III.4)}$$

and the condition is

$$\frac{\partial R}{\partial a} = 0; \quad \frac{\partial R}{\partial b} = 0. \qquad \text{(III.5)}$$

This results in

$$a = \frac{\Sigma y_i}{k} \qquad \text{(III.6)}$$

and

$$b = \frac{\Sigma(x_i - \bar{x})y_i}{\Sigma(x_i - \bar{x})^2}\ , \qquad \text{(III.7)}$$

where k is the number of observations, $(x_1,y_1),(x_2,y_2)$, ..., (x_k,y_k), and $\bar{x}$ is the average of x_i. The root mean square deviation (RMS) is given by

$$RMS = \sqrt{\frac{R}{k}}\ . \qquad \text{(III.8)}$$

We have considered the linewidth (peak-to-peak width of the derivative signal) to the corresponding Zeeman-field intensity, for two types of variation, viz.,linear (H) and quadratic (H^2). These equations are,

(a) for the linear variation,

$$\Delta H = a + bH\ , \text{ and} \qquad \text{(III.9)}$$

(b) for the quadratic variation,

$$\Delta H = c + dH^2. \qquad \text{(III.10)}$$

The results are presented in Chapters VI and VII.

REFERENCES

1. 'V-4502 EPR Spectrometer System Manual' Varian Associates, California.

2. A. Holden and P. Singer, 'Crystals and Crystal Growing', Doubleday and Co., New York (1968).

3. B. Bleaney and D.J.E. Ingram, Proc. Roy. Soc. (London) A205, 336 (1951).

4. J.G. Chambers, W.R. Datars, and C. Calvo, J. Chem. Phys. 41, 806 (1964).

5. K.D. Bowers and J. Owen, in 'Reports on Progress in Physics' (Ed. A.C. Stickland) Vol.18, p.304. Published by the Physical Society, London (1955).

6. K.A. Brownlee, 'Statistical Theory and Methodology in Science and Engineering', John Wiley and Sons, New York (1965).

CHAPTER IV

ELECTRON PARAMAGNETIC RESONANCE OF Mn^{2+} IN ZINC ACETATE DIHYDRATE*

Abstract

Electron paramagnetic resonance of Mn^{2+} ion in monoclinic zinc acetate dihydrate $[Zn(CH_3COO)_2 \cdot 2H_2O]$ has been studied at room temperature. The Mn^{2+} ion, substituting for the Zn^{2+} sites in the tetramolecular unit cell of $Zn(CH_3COO)_2 \cdot 2H_2O$, exhibited the characteristic 30 line absorption spectrum, indicating that all the sites which Mn^{2+} entered are magnetically equivalent. The spectra for the Zeeman-field direction along the principal axes have been analyzed for the spin-Hamiltonian constants. Besides the allowed ($\Delta M = \pm 1, \Delta m = 0$) transitions, hyperfine-forbidden ($\Delta M = \pm 1$, $\Delta m = \pm 1$) transitions have been observed, when the Zeeman-field direction was off from either the principal z axis or the principal xy plane. From the doublets' separation of the forbidden transitions for the $M = +1/2 \leftrightarrows -1/2$ transition, the quadrupole constants for Mn^{2+} in this system were calculated.

---

* The contents of this chapter have been published in J. Physics Chem. Solids 31, 1419 (1970).

Introduction:

The EPR studies of both undiluted and diluted manganese acetate [$Mn(CH_3COO)_2 \cdot nH_2O$] have been carried out earlier. The EPR of undiluted $Mn(CH_3COO)_2 \cdot 4H_2O$ was studied by Abe and Morigaki.[1] Kumugai et al.,[2] and Hayashi and Ono[3] reported the EPR of $Mn(CH_3COO)_2 \cdot 3H_2O$ diluted in isostructural zinc acetate trihydrate [$Zn(CH_3COO)_2 \cdot 3H_2O$]. In this chapter we report the EPR of Mn^{2+} in zinc acetate dihydrate [$Zn(CH_3COO)_2 \cdot 2H_2O$].

Crystal Structure:

The crystal structure of $Zn(CH_3COO)_2 \cdot 2H_2O$ was reported by van Niekerk, Schoening, and Talbot.[4] The unit cell is monoclinic with dimensions

$$a_o = 14.50 \text{ Å}, \quad b_o = 5.32 \text{ Å}, \quad c_o = 11.02 \text{ Å}, \text{ and}$$
$$\beta = 100^\circ 0'.$$

The four formula units in the tetramolecular unit cell are derived by the operation of the space group C2/c. The projection of the unit cell along its b_o axis is shown in Fig. IV-1.[5] For C2/c space group, the equivalent atoms or molecules are in the following positions:

$$\pm(0,u,\tfrac{1}{4};\ \tfrac{1}{2},u+\tfrac{1}{2},\tfrac{1}{4})$$

for zinc atoms (u = 1/8.3), and

$$\pm(x,y,z;\ x,\bar{y},z+\tfrac{1}{2};\ x+\tfrac{1}{2},y+\tfrac{1}{2},z;\ x+\tfrac{1}{2},\tfrac{1}{2}-y,z+\tfrac{1}{2})$$

for other atoms or molecules. The zinc atoms lie on a two-fold

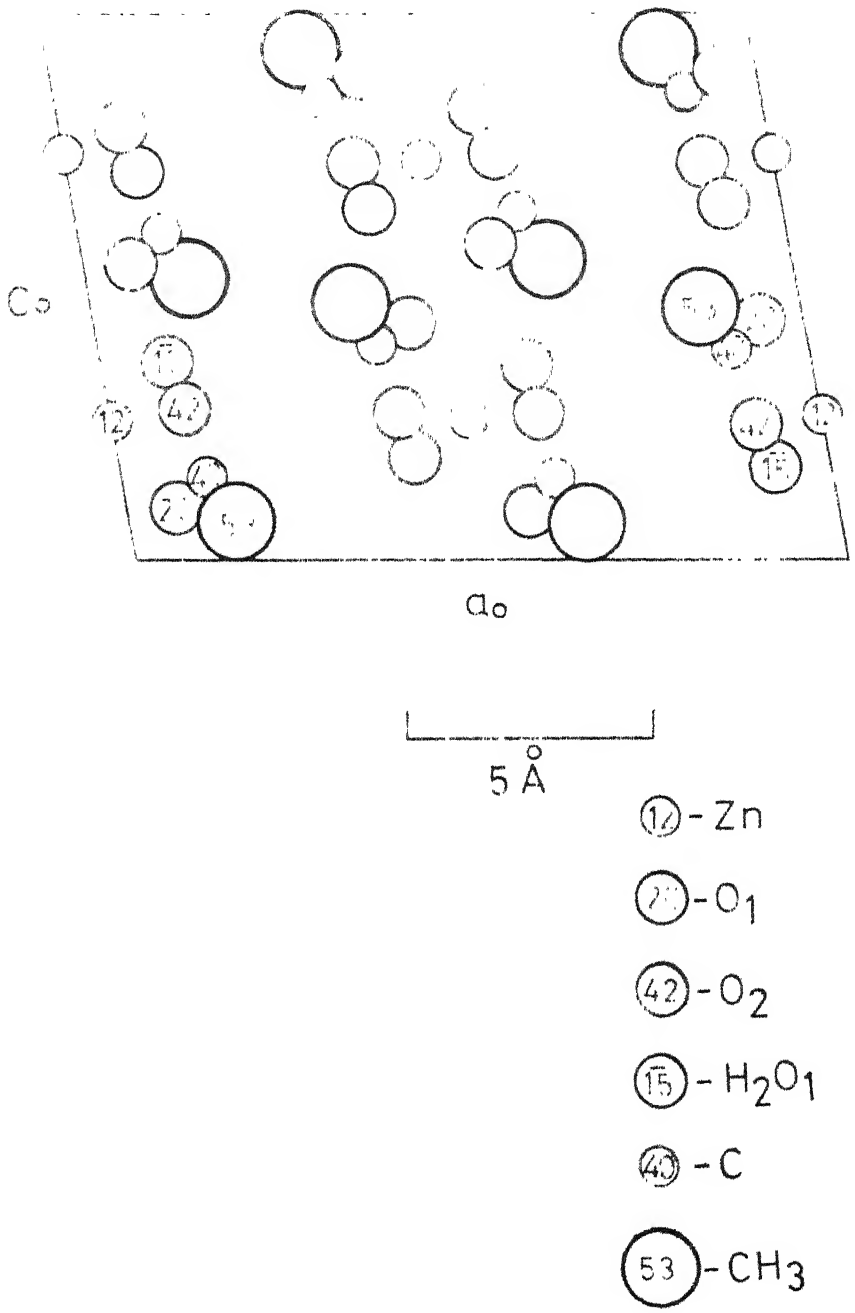

Fig. IV-1: The monoclinic crystal structure of $Zn(CH_3COO)_2 \cdot 2H_2O$ projected along its b_o axis. The numbers inside the circles represent the positions of the atoms or molecules along the b_o axis in units of the unit cell dimension along the b_o axis (100 = 5.32 Å).

axis parallel to the b axis. The six nearest neighbors of a zinc atom, forming a greatly distorted octahedron, are, two oxygen atoms (O_1 and O_1^o) at a distance 2.17 Å, two more oxygen atoms of the two acetate groups (O_2 and O_2^o) at 2.18 Å, and the two water molecules (H_2O and H_2O^o) at 2.14 Å. The atoms or molecules with the superscript 'o' are obtained from the corresponding non-superscripted ones by a two-fold rotation parallel to the b axis through the zinc atom. These nearest neighbors subtend angles at Zn^{2+} as given below:

$$O_1\text{-}Zn\text{-}O_1^o = 158^o, \quad O_2\text{-}Zn\text{-}O_2^o = 85^o, \text{ and}$$
$$H_2O\text{-}Zn\text{-}H_2O^o = 94^o.$$

The single crystals of $Zn(CH_3COO)_2 \cdot 2H_2O$ grow as thin plates parallel to bc plane.[4]

Results and Discussion:

a. Allowed transitions:

The EPR of Mn^{2+} in $Zn(CH_3COO)_2 \cdot 2H_2O$ has been studied at room temperature. The spectra for the Zeeman-field direction along the three principal axes are shown in Figs. IV-2 to 4. These have been analyzed for the spin-Hamiltonian constants (as described in Chapter III), and these are,

$g_z = 2.0013 \pm 0.001$, $g_x = 2.0014 \pm 0.001$, $g_y = 2.0024 \pm 0.001$, $D = +248.0 \pm 0.5G$, $E = -25.5 \pm 1.5G$, $A_z = -89.6 \pm 0.5G$, $A_x = -89.9 + 0.5G$, and $A_y = -89.3 \pm 0.5G$.

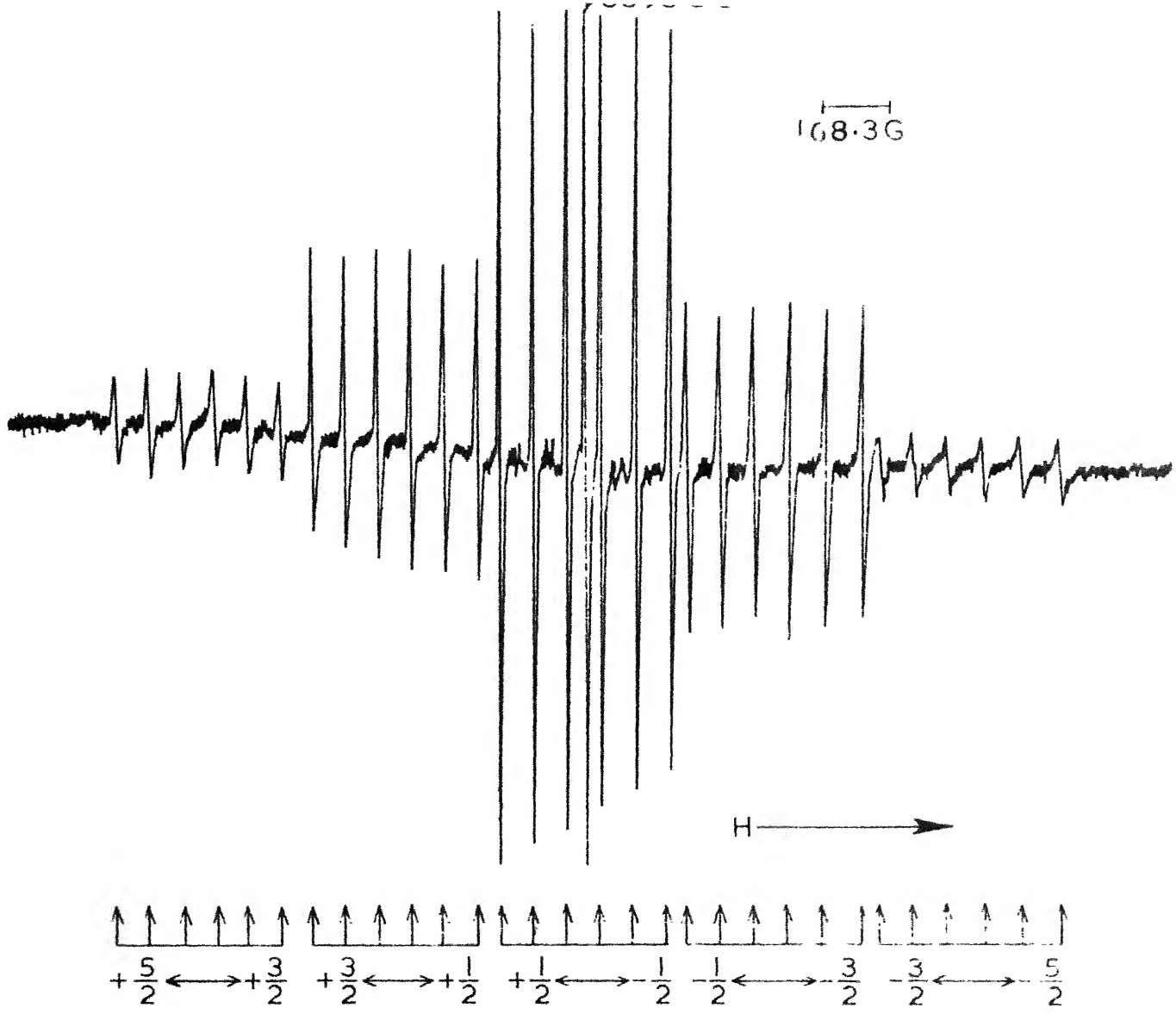

Fig. IV-2: The EPR spectrum of Mn^{2+} in $Zn(CH_3COO)_2 \cdot 2H_2O$ [illegible] direction along the z axis.

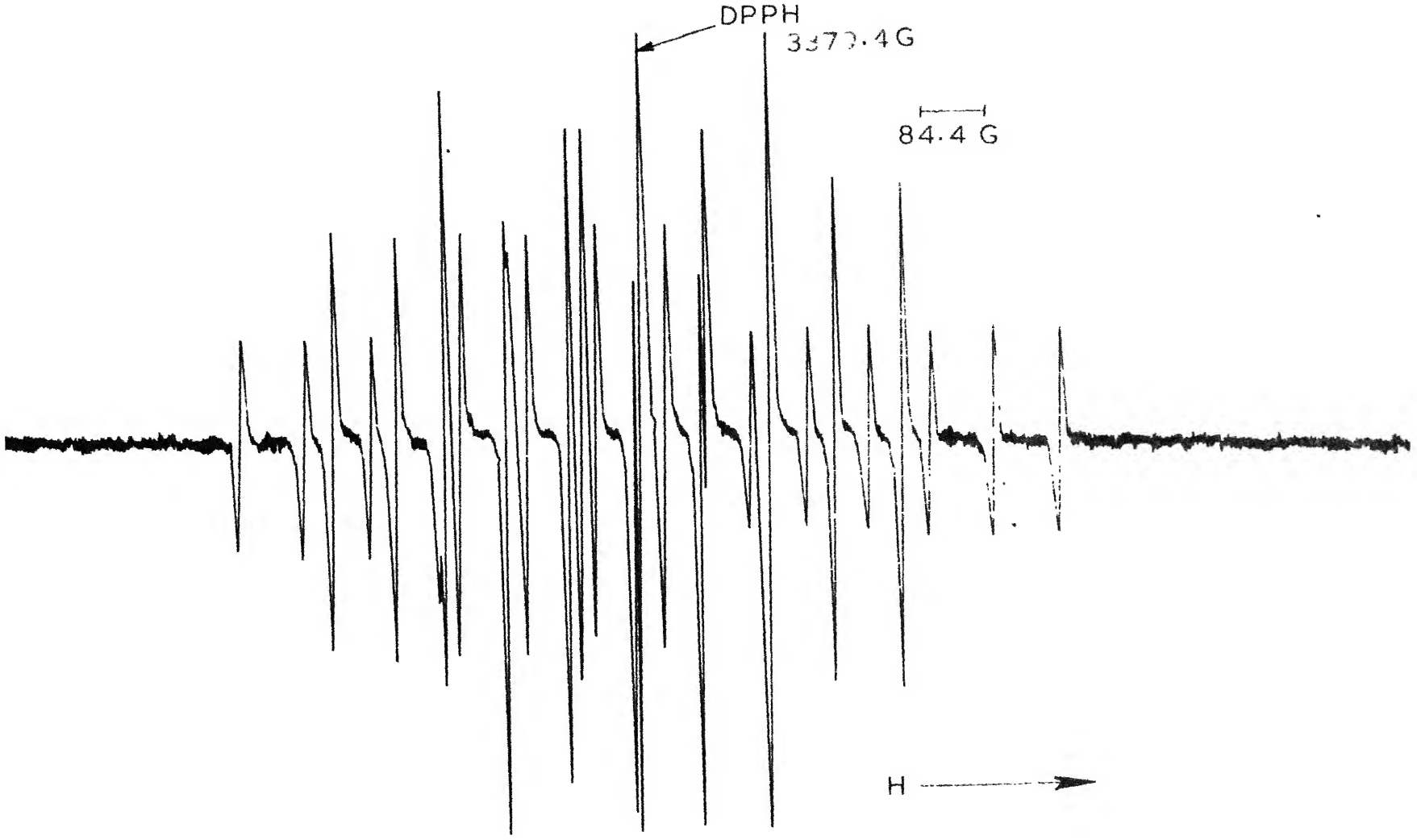

Fig. IV-3· The EPR spectrum of M[illegible] direction along the [illegible]

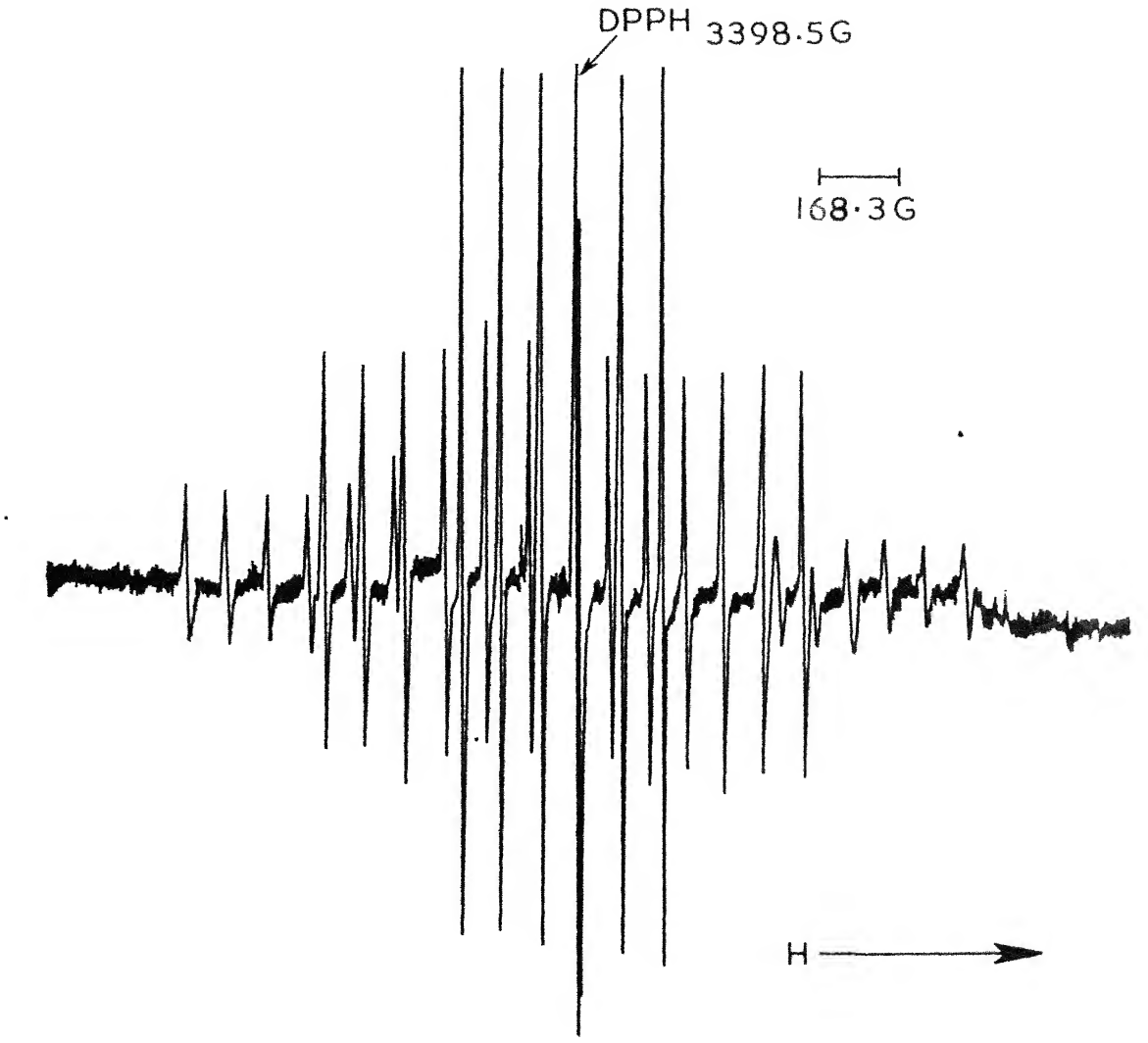

Fig. IV-4: The EPR spectrum of Mn^{2+} in $Zn(CH_3COO)_2 \cdot 2H_2O$ for the Z[illegible] direction along the x axis.

For the Zeeman-field direction along the three principal axes only one group of 30 ($\Delta M = \pm 1, \Delta m = 0$) transitions has been observed. From the space group operation relating the four molecules within the unit cell, and considering Zn^{2+} to be the origin, it is easily seen that the four molecules are identical in pairs, one obtained from the other by a reflection in the crystallographic ac plane. This reflection symmetry about the ac plane, and the two-fold rotational symmetry within each $Zn(CH_3COO)_2 \cdot 2H_2O$ molecule about the b axis, make, as far as the phenomenon of magnetic resonance is concerned, all the four Zn^{2+} sites identical. Thus the EPR of Mn^{2+}, which substitutes for Zn^{2+} in $Zn(CH_3COO)_2 \cdot 2H_2O$ exhibits only one group of 30 allowed transitions. Similar observations have been made in Mn^{2+}-doped, tetramolecular calcium tungstate ($CaWO_4$, space group $I4_1/a$)[6] and pyroxene diopside ($CaMgSi_2O_6$, space group C2/c),[7] where also the reflection symmetry of the four molecules about a plane and the two-fold rotational symmetry within a molecule about an axis perpendicular to this plane contributed to the appearance of a single group of allowed transitions, for Mn^{2+} substituting the divalent cations. The y axis of the principal system of axes coincided with the two-fold symmetry axis (crystallographic b axis).

The linewidths (peak-to-peak width of the derivative signal) were of the order of 7G, while the sharpest line had

a width of about 3G. This smallness of the linewidth is due to the fact that four of the six ligands surrounding Mn^{2+}, substituting for Zn^{2+}, are oxygen atoms, which do not contribute to the dipolar interaction between the paramagnetic ion and the spins of the ligand nucleus, because of their zero nuclear spin.

The linewidths of the different fine-structure transitions were not same, those of M = + 1/2 $\leftrightarrow$ - 1/2 transition being the smallest and increasing with the transitions involving larger quantum numbers of M. This variation of linewidth with the fine-structure transition has been observed to be minimum along the crystallographic b axis. This feature has been previously observed,[6,8] and has been explained by Vanier.[8] The magnetic field for a fine-structure transition (for the simple case of axial symmetry) is given by

$$H = H_o + (2M - 1)D(3\cos^2\theta - 1), \qquad (IV.1)$$

where M is the quantum number for the transition $M \rightarrow M \pm 1$ and θ is the angle between the z axis and the Zeeman-field direction. Statistical fluctuations in the local crystalline field due to crystalline imperfections are reflected as fluctuations in the amplitudes of D and θ (due to statistical fluctuations in the orientation of the axis of symmetry of the complexes). The larger dependence of the resonance field values, of transitions involving larger quantum numbers of M, on D, because of the multiplication factor 2M-1, and on θ,

because of the strong angular variation of these transitions, results in larger linewidths for these transitions due to crystalline imperfections.

b. Hyperfine-forbidden transitions:

The intensity of the allowed transitions decreased very rapidly as the direction of the Zeeman field was changed from either the z axis or the xy plane, and simultaneously hyperfine-forbidden ($\Delta M = \pm 1$, $\Delta m = \pm 1$) transitions have been observed to increase in intensity. These appear as doublets between the ($\Delta M = \pm 1$ $\Delta m = 0$) transitions for the $M = 1/2 \leftrightarrow -1/2$ transition.[9]

Hyperfine-forbidden transitions have been observed in many systems, of cubic,[9-11] axial,[12-17] and orthorhombic[18] symmetries. These appear when the Zeeman-field direction is off the z axis. The occurrence of these transitions has been explained as due to second order mixing of the hyperfine constant A, with the fine-structure constant a, D, or D and E, for the cases of cubic, axial, or orthorhombic symmetries. Bleaney and Ingram,[12] who first observed these transitions, attributed them to the breakdown of the selection rule $\Delta m = 0$, when the Zeeman-field direction is very much off the z axis, and when the quadrupole interaction term (Q') is comparable with B. Later Ludwig and Woodbury,[19] and Bleaney and Rubins,[20] explained the occurrence of these transitions as due to the second order mixing of S and I, of the form $S_{\pm}I_{\mp}$ ($S_{\pm} = S_x \pm iS_y$

and $I_{\pm} = I_x \pm iI_y$). The intensities of these transitions relative to the allowed transitions have been calculated by Friedman and Low,[9] and Bleaney and Rubins.[20] According to these authors, the intensity variation is of the form $D^2\sin^2\theta\cos^2\theta/A^2$,[9] and $D^2\sin^2\theta\cos^2\theta/(g\beta H)^2$,[20] where θ is the angle between the z axis and the Zeeman-field direction. But in some cases,[21] and also in the present case, the relative intensity variation has been observed to be very much larger than predicted by the above expressions. For our case, the intensity of the forbidden transitions relative to the allowed transitions for different values of θ, in the zx plane, is given in Fig. IV-5. For $\theta > 15^{\circ}$, the forbidden-transition intensities were very much stronger than those of the allowed transitions. The strong intensity variation of the allowed and forbidden transitions with θ has been explained by Bir.[22] For paramagnetic ions with $S > 1/2$ and $I \neq 0$ placed in a crystalline field, the hyperfine-structure transitions occur as a combination of a transition of the electrons in the ion and the nuclear spins from one state to another. Since the effective magnetic field associated with the hyperfine interaction is much greater compared to the Zeeman field, the quantization axis for nuclear spins is the direction of the effective field. This effective field is determined by the state of the electrons in the ion and θ, and hence is not along the Zeeman-field direction when off the axes. The functional dependence between the direction of quantization axes

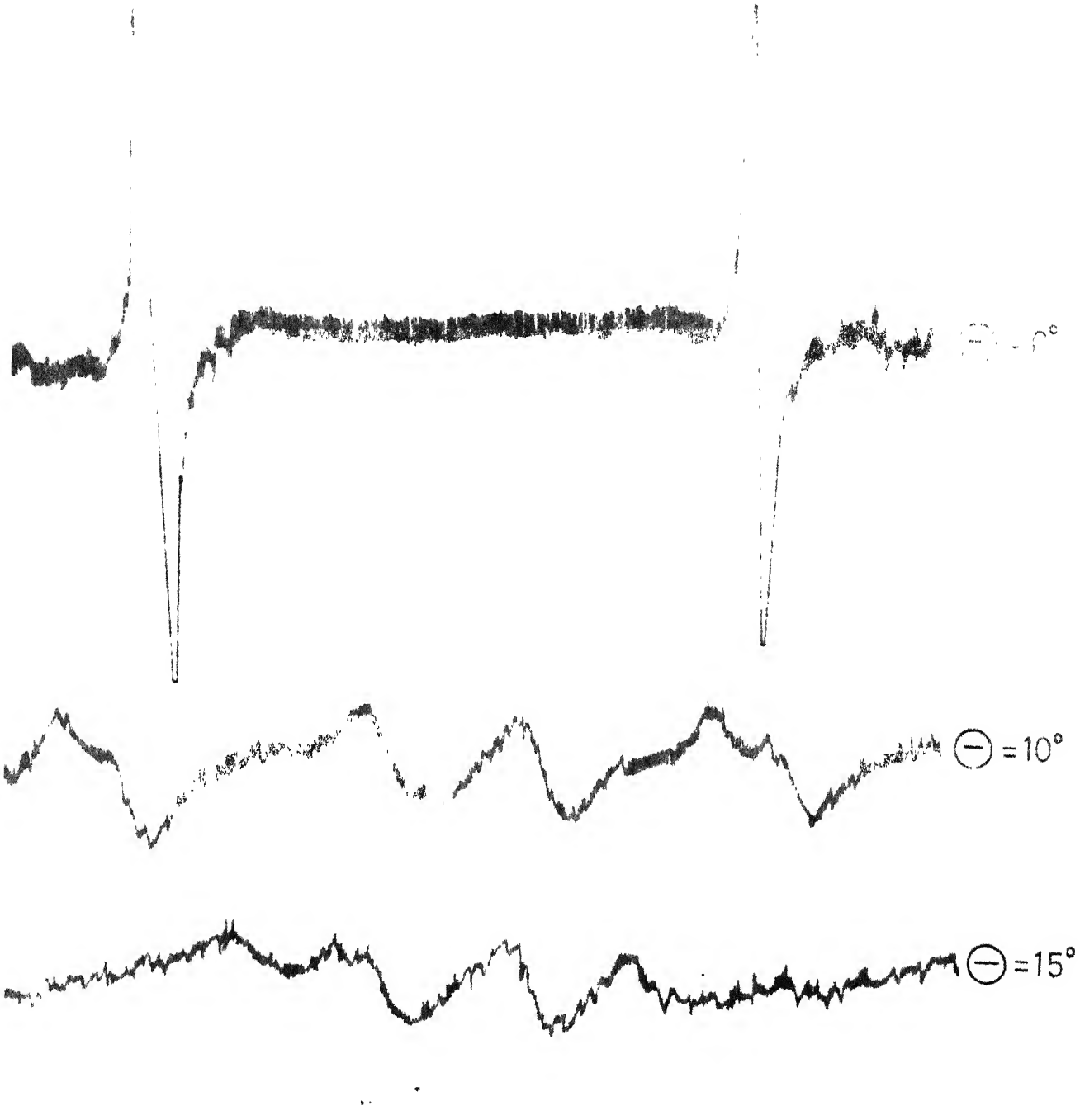

Fig. IV-5: The intensity of the hyperfine-forbidden ($\Delta M = \pm 1$, $\Delta m = \pm 1$) transitions relative to the allowed ($\Delta M = \pm 1$, $\Delta m = 0$) transitions for the Zeeman-field direction making 0°, 10°, and 15° with the z axis in the zx plane. The allowed transitions are the $m = -1/2 \rightleftarrows -1/2$ and $+1/2 \rightleftarrows +1/2$ transitions of $M = +1/2 \rightleftarrows -1/2$.

and the electron states leads to lack of orthogonality between various nuclear spin projections and the nuclear spin functions. The overlap of the nuclear spin functions, along with the transition between the initial and final states of the ion, contributes to the matrix element of a hyperfine-structure transition, and leads to the occurrence of hyperfine-forbidden transitions. The overlap integral of the nuclear spin functions is very strongly dependent on the angle between the quantization axes for different states of the electron, which is the reason why the intensity of the hyperfine-structure transitions is so strongly dependent on θ.

The hyperfine ($\Delta M = \pm 1$, $\Delta m = \pm 1$) forbidden transitions appear as doublets between the ($\Delta M = \pm 1, \Delta m = 0$) transitions of the $M = +1/2 \mp -1/2$, transition. The separation between these doublets is given by[18]

$$H = \frac{17B^2}{H_o} + \left[\frac{2\gamma\beta_N}{g\beta}\right]H - \left[Q'(3\cos^2\theta - 1) + 3Q''\sin^2\theta\cos 2\phi\right]$$

$$x(2m + 1) + \left[\frac{4B^2D}{H_o^2}(3\cos^2\theta - 1) - \frac{25A^3}{2H_o^2}\right](2m + 1), \quad (IV.2)$$

where γ is the gyromagnetic ratio of the Mn^{55} nucleus, β_N is the nuclear magneton, θ and ϕ are the polar angles, and B is the average of A_x and A_y. $m = -5/2$ corresponds to the doublets occurring between $m = -5/2$ and $m = -3/2$ allowed transitions, etc., and Q' and Q" are as given in Eq. (II.19). The doublets between the allowed transitions for the Zeeman-field direction

making an angle of $\theta = 10^{\circ}$, in the zx plane ($\phi = 0^{\circ}$), with the z axis are shown in Fig. IV-6. From the doublets' separations at angles $\theta = 10^{\circ}$ and 15° from z axis in the zx plane, Q' and Q" have been calculated, and these are

$$Q' = 0.40G \quad \text{and} \quad Q'' = 4.7G.$$

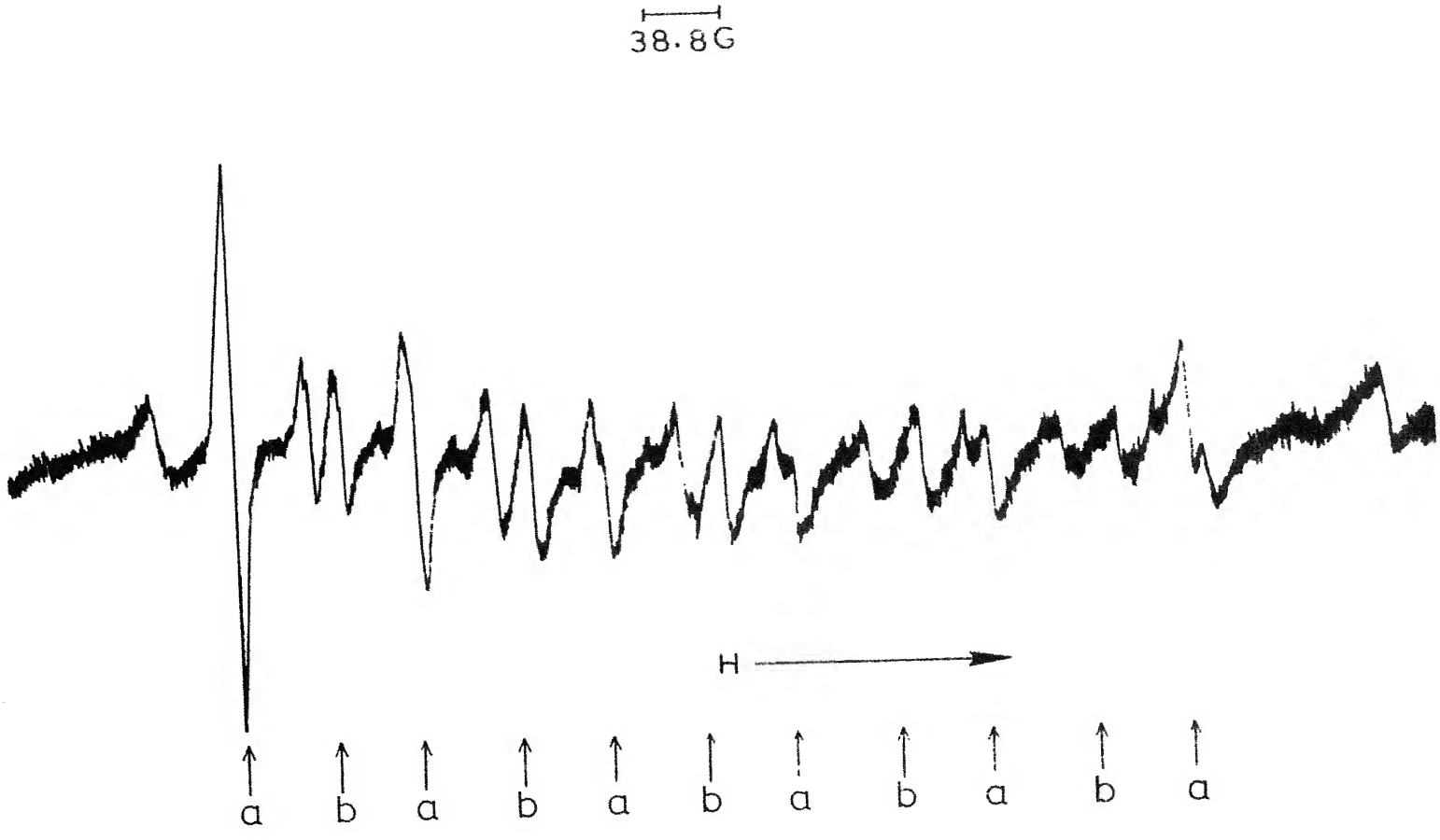

Fig. IV-6 The [illegible] for the Zeeman-[illegible] in the [illegible] transitions are marked [illegible] tions are marked [illegible].

REFERENCES

1. H. Abe and H. Morigaki, in 'Paramagnetic Resonance' (Ed. W. Low) Vol. 2, p.567. Academic Press, New York (1963).

2. H. Kumugai, K. Ono, I. Hayashi, and K. Kambe, Phys. Rev. 87, 374 (1952).

3. I. Hayashi and K. Ono, J. phys. Soc. Japan 8, 270 (1953).

4. J.N. van Niekerk, F.R.L. Schoening, and J.H. Talbot, Acta crystallogr. 6, 720 (1953).

5. R.W.G. Wyckoff, 'Crystal Structures', Vol. 5, p.329. Interscience, New York (1966).

6. C.F. Hempstead and K.D. Bowers, Phys. Rev. 118, 131 (1960).

7. V.M. Vinokurov, M.M. Zaripov, and V.G. Stepanov, Soviet Phys. solid St. 6, 870 (1964).

8. J. Vanier, Can. J. Phys. 42, 494 (1964).

9. E. Friedman and W. Low, Phys. Rev. 120, 408 (1960).

10. J.E. Drumheller and R.S. Rubins, ibid. 133, A1099 (1964).

11. G.J. Wolga and R. Tseng, ibid. 133, A1563 (1964).

12. B. Bleaney and D.J.E. Ingram, Proc. Roy. Soc. (London) A205, 336 (1951).

13. L.M. Matarrese, J. Chem. Phys. 34, 306 (1961),

14. F. Waldner, Helv. phys. Acta 35, 756 (1962).

15. V.J. Folen, Phys. Rev. 125, 1581 (1962).

16. J. Schneider and S.R. Sircar, Z. Naturf. 17a, 651 (1962).

17. S.P. Burley, Aust. J. Phys. 17, 537 (1964).

18. K.N. Shrivastava and P. Venkateswarlu, Proc. Indian Acad. Sci. 63, 311 (1966).

19. G.W. Ludwig and H.H. Woodbury, Bull. Am. phys. Soc. ser II 5, 156 (1960).

20. B. Bleaney and R.S. Rubins, Proc. phys. Soc. (London) 77, 103 (1961) and 78, 778 (1961).

21. M.I. Kornfeld and L.S. Sochava, Soviet Phys. solid St. 5, 1625 (1964).

22. G.L. Bir, ibid. 5, 1628 (1964).

CHAPTER V

ELECTRON PARAMAGNETIC RESONANCE OF Mn^{2+} IN FERROUS AMMONIUM SULFATE HEXAHYDRATE*

Abstract

Electron paramagnetic resonance of Mn^{2+} ion has been studied in ferrous ammonium sulfate hexahydrate [$Fe(NH_4)_2(SO_4)_2 \cdot 6H_2O$] from room temperature till 77°K. The Mn^{2+} ion was found to substitute for Fe^{2+} and exhibit two inequivalent magnetic complexes corresponding to the two Fe^{2+} sites in the unit cell of $Fe(NH_4)_2(SO_4)_2 \cdot 6H_2O$. From room temperature till 77°K, no noticeable effect of Fe^{2+} on the EPR of Mn^{2+} has been observed. The spin-Hamiltonian constants of Mn^{2+} in this system have been compared with the corresponding parameters of Mn^{2+} in isostructural compounds. This comparison gives a qualitative idea about the coordination of the octahedron of the six water molecules surrounding Fe^{2+} in $Fe(NH_4)_2(SO_4)_2 \cdot 6H_2O$, whose detailed crystal structure has not been studied so far.

---

* The contents of this chapter have been published in Chem. phys. Lett. 4, 550 (1970).

Introduction:

To obtain the details of the interaction of a paramagnetic ion (like the fine-structure and hyperfine-structure interactions) in an EPR spectrum, the interaction between the paramagnetic ions is reduced by using magnetically dilute mixed crystals, where most of the paramagnetic ions are replaced by diamagnetic ions.[1] Further it has been observed[2,3] that the paramagnetic ions whose spin-lattice relaxation time is short at room temperature can also be used in place of the diamagnetic ions, till high enough temperatures so that the spin-lattice relaxation time of the diluting ion does not approach the Larmor precession period of the resonating paramagnetic ion. The ions which belong to this class are, most of the paramagnetic rare earth ions excepting Gd^{3+} and Eu^{2+}, and Ti^{3+}, V^{3+}, Fe^{2+}, and Co^{2+} in the iron group series.[4] Using these rare earth ions as the diluting ions, the EPR of Gd^{3+} has been studied at room temperature by Upreti[5] and Singh et al.[6-10] The present and the subsequent two chapters deal with the EPR of Mn^{2+}, where the diluting ions are Fe^{2+} and Ni^{2+} respectively. This type of study is useful in two ways. Firstly, the effect of the diluting ions on the EPR of Mn^{2+} can be studied, and secondly, the EPR of Mn^{2+} can be used as an effective probe to reveal the symmetry and strength of the crystalline field at the Mn^{2+} ions doped in these lattices. This is specially interesting since the detailed crystal

[illegible] ammonium sulfate hexahydrate [$Fe(NH_4)_2(SO_4)_2 \cdot$ [illegible], hereafter abbreviated as FASH], which belongs to a group of isostructural compounds - called Tutton's salts, has not been studied, to the best of our knowledge.

Tutton's salts have been studied by EPR since the early days[11,12] mainly in salts where Ni^{2+} and Cu^{2+} are the divalent cations,[13,14*] and in Mn^{2+}-doped magnesium ammonium sulfate hexahydrate [$Mg(NH_4)_2(SO_4)_2 \cdot 6H_2O$],[15,16] and zinc ammonium sulfate hexahydrate [$Zn(NH_4)_2(SO_4)_2 \cdot 6H_2O$].[17,18] Though the overall unit cell symmetry and the space group are same for all the Tutton's salts, the distances and relative orientations of the ligands around the divalent cation for the two sites in the bimolecular unit cell may vary.

Crystal Structure:

FASH belongs to a group of isostructural compounds, called Tutton's salts. The general chemical formula of a Tutton's salt is of the form $M'' M'_2(XO_4)_2 \cdot 6H_2O$, where M'' is a divalent cation, like Mg^{2+}, Zn^{2+}, Fe^{2+} etc., M' is a monovalent cation, like $(NH_4)^+$, K^+ etc., and X is S or Se. The unit cell symmetry of the Tutton's salt is monoclinic and has two molecules related by the operation of the space group $P2_1/a$.[19,20] An x-ray study of the structure determination of these salts was made by Hoffman.[21] However, of the many compounds, detailed crystal structure has been studied

* These references do not form a complete list. Only a few are quoted for general reference.

...ly for now, viz., $Ni(NH_4)_2(SO_4)_2 \cdot 6H_2O$,[22] $Zn(NH_4)_2(SO_4)_2 \cdot 6H_2O$,[22] ... $Mn(NH_4)_2(SO_4)_2 \cdot 6H_2O$.[22] The unit cell dimensions of FASH, ... of $Mg(NH_4)_2(SO_4)_2 \cdot 6H_2O$ and $Zn(NH_4)_2(SO_4)_2 \cdot 6H_2O$ are given hereunder. These are,[20]

for FASH:

$$a_o = 9.30 \text{ Å}, \quad b_o = 12.60 \text{ Å}, \quad c_o = 6.23 \text{ Å},$$

$$\text{and } \beta = 106^\circ 50',$$

for $Mg(NH_4)_2(SO_4)_2 \cdot 6H_2O$:

$$a_o = 9.324 \text{ Å}, \quad b_o = 12.597 \text{ Å}, \quad c_o = 6.211 \text{ Å},$$

$$\text{and } \beta = 107^\circ 8',$$

and for $Zn(NH_4)_2(SO_4)_2 \cdot 6H_2O$:

$$a_o = 9.233 \text{ Å}, \quad b_o = 12.500 \text{ Å}, \quad c_o = 6.237 \text{ Å},$$

$$\text{and } \beta = 106^\circ 52'.$$

The projection of the unit cell of one of the Tutton's salts, viz., $Mg(NH_4)_2(SO_4)_2 \cdot 6H_2O$, along its c_o axis is shown in Fig. V-1.[20] The divalent cations are at the positions,

$$(0,0,0) \quad \text{and} \quad (\tfrac{1}{2},\tfrac{1}{2},0),$$

while the other atoms and molecules are at,

$$\pm(x,y,z) \quad \text{and} \quad \pm(x+\tfrac{1}{2}, \tfrac{1}{2}-y, z).$$

The divalent ion is surrounded by an octahedron of six water molecules.

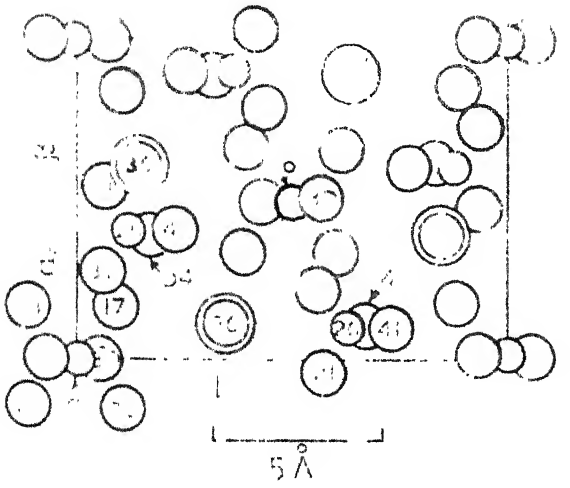

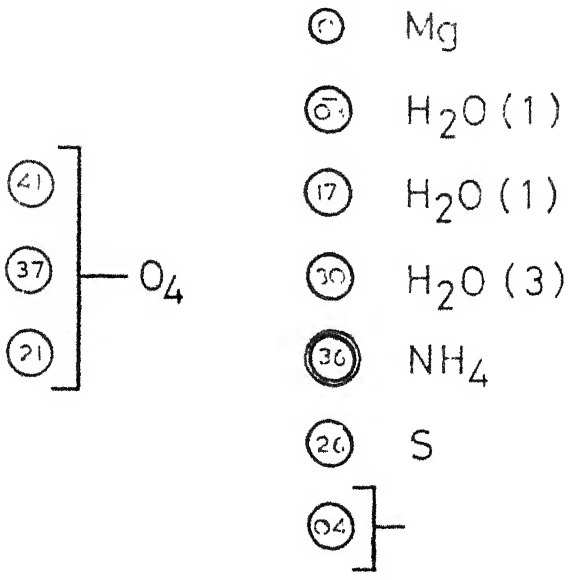

Fig. V-1. The monoclinic crystal structure of $Mg(NH_4)_2(SO_4)_2 \cdot 6H_2O$ projected along its c_0 axis. The numbers inside the circles represent the positions of the atoms or molecules along the c_0 axis in units of the unit cell dimension along the c_0 axis (100 = 6.271 Å). For the other molecule of the unit cell, the positions of Mg and $H_2O(3)$ are given.

Results and Discussion:

The EPR of Mn^{2+} in FASH has been studied at room temperature. The spectrum exhibited the characteristic magnetic inequivalency for the Mn^{2+} ions, which go substitutionally to Fe^{2+} in the bimolecular unit cell of FASH. The z axes of the two magnetically inequivalent complexes have been obtained by obtaining maximum spread of the fine-structure separation. The EPR spectrum for the Zeeman-field direction along the z axis of one of the complexes of Mn^{2+} is shown in Fig. V-2. This has been analyzed for the spin-Hamiltonian constants (as described in Chapter III), and these are,

$$g_z = 2.0037 \pm 0.001, \quad D = -248.2 \pm 0.5G,$$
$$A = -94.0 \pm 0.5G, \quad |E| = 49 \pm 5G, \text{ and } |B| = 98 \pm 5G.$$

Iron^{2+} has a $(3d)^6$ outershell configuration and a ground state $^5D_4$. The five-fold orbital degeneracy is lifted in a crystalline field of cubic symmetry into a low-lying doublet and a triplet. Terms of orthorhombic symmetry in the crystalline field lift the orbital degeneracy completely. The action of the spin-orbit interaction removes the spin degeneracy leaving the ground state a doublet with the other levels lying several cm^{-1} above. Thus the effective spin of Fe^{2+} is 1/2. The spin-lattice relaxation time of Fe^{2+} is very small at room temperature and the observation of EPR of Fe^{2+} requires very low temperatures.[12]

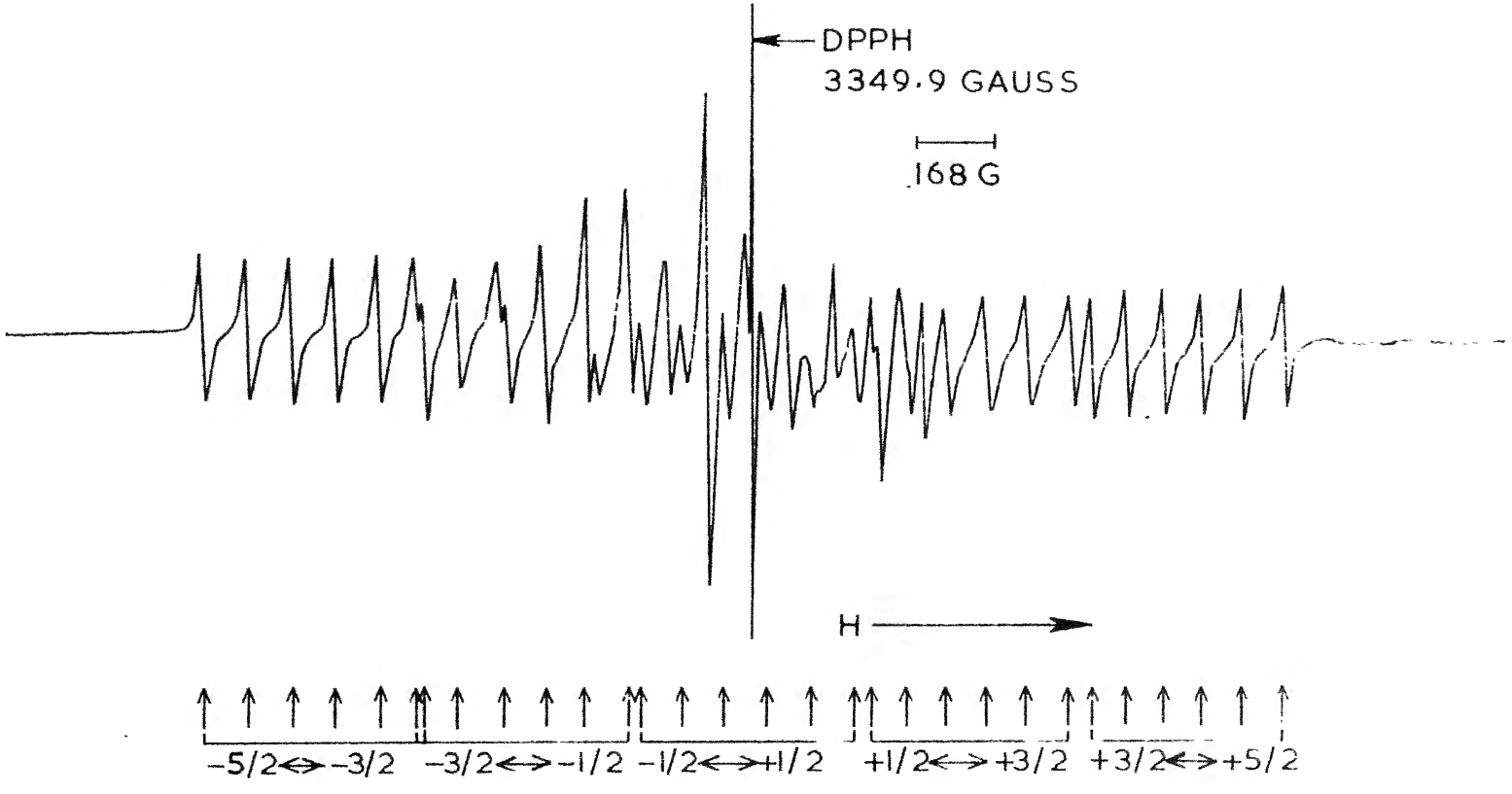

Fig. V-2: The EPR spectrum of Mn^{2+} in $Fe(NH_4)_2(SO_4)_2 \cdot 6H_2O$ for the [illegible] along the z axis of one of the magnetic complexes of Mn^{2+}.

At room temperature the linewidths of the EPR spectrum of Mn^{2+} in FASH were of the order of 10G, characteristic of those in a diluted diamagnetic hydrated lattice. The EPR has also been studied in the temperature range 300°K-77°K. No noticeable effect has been observed, either in the linewidths or in the g value. The EPR of Fe^{2+} in FASH was observed at 20°K.[24] Thus at temperatures where the spin-lattice relaxation time is smaller than the Larmor precession period of Mn^{2+}, the effect of Fe^{2+} on Mn^{2+} is not felt. This explains the observation, in the temperature range studied, of the linewidths of Mn^{2+} in FASH like those in a diamagnetic hydrated lattice.

Our observations are compared with the EPR studies of Mn^{2+} in other Tutton's salts. This gives a qualitative idea of the local symmetry at Fe^{2+}, especially in the system where no detailed crystal structure is available. The comparison is given in Table V-1.

In all the salts quoted in the Table V-1, D and E are very nearly of the same magnitude. Thus qualitatively it can be concluded that the coordination of octahedron of water molecules at the divalent cation is nearly same for all the three systems, both as regards to the symmetry and the distances from the divalent cation.

The angle between the z axes of the two magnetically inequivalent Mn^{2+} complexes in FASH has been found to be $70\pm5°$. In the case of Mn^{2+} in $Zn(NH_4)_2(SO_4)_2 \cdot 6H_2O$,[17] this angle has

TABLE V-1

Spin-Hamiltonian Parameters of Mn^{2+} in Tutton's Salts at Room Temperature*,+

Host Lattice	D	E	A	B	Reference
	(in units of $cm^{-1} \times 10^{-4}$)				
$Mg(NH_4)_2(SO_4)_2 \cdot 6H_2O$	231	60	90	90	[15]
$Zn(NH_4)_2(SO_4)_2 \cdot 6H_2O$	243	100	-91	-91	[17]
$Fe(NH_4)_2(SO_4)_2 \cdot 6H_2O$	-232.5	45	-89	91	[Present study]

* Ono and Hayashi[3] have observed the EPR of Mn^{2+} in Fe, Ni, and Co ammonium sulfates, hexahydrate, but no parameters are given.

\+ Only the EPR of Mn^{2+} is tabulated, though other divalent ions like Cu^{2+} have also been studied.

been reported to be 64°. In the case of Mn^{2+} in $Mg(NH_4)_2(SO_4)_2 \cdot 6H_2O$,[15] it has been reported that two maxima were observed, one each in K_AK_3 and K_BK_3 planes, at approximately 30° from either K_A or K_B. If these two maxima correspond to the directions of the Zeeman field along the z axes of the inequivalent Mn^{2+} sites, then the corresponding angle is 75°. All these angles are almost of the same magnitude, which indicates that FASH has very nearly the same configuration of ligand water molecules as in the other two Tutton's salts. The calculated angle between the two z axes in the case of $Mg(NH_4)_2(SO_4)_2 \cdot 6H_2O$,[22] assuming that the distortion is along Mg-O, where O is the oxygen ion of the H_2O which is nearest to Mg, comes out to be 70°.

REFERENCES

1. B. Bleaney and D.J.E. Ingram, Proc. phys. Soc. (London) A63, 408 (1950).

2. B. Bleaney, R.J. Elliott, and H.E.D. Scovil, ibid. A64, 933 (1951).

3. K. Ono and I. Hayashi, J. phys. Soc. Japan 8, 561 (1953).

4. D.M.S. Bagguley, B. Bleaney, J.H.E. Griffiths, R.P. Penrose, and B.I. Plumpton, Proc. phys. Soc. (London) 61, 542 (1948).

5. G.C. Upreti, Ph.D. Thesis, Department of Physics, Indian Institute of Technology, Kanpur (1966).

6. G.P. Singh and P. Venkateswarlu, Proc. Indian Acad.Sci. 65, 211 (1967).

7. G.P. Singh and P. Venkateswarlu, ibid. 65,361 (1967).

8. G.P. Singh and G.C. Upreti, ibid. 66, 104 (1967).

9. G.P. Singh, G.C. Upreti, and P. Venkateswarlu, J. Chem. Phys. 46, 2885 (1967).

10. G.P. Singh and P. Venkateswarlu, ibid. 46,4765 (1967).

11. S. Altshuler and B.M. Kozyrev, 'Electron Paramagnetic Resonance', Ch. 4, Academic Press, New York (1964).

12. K.D. Bowers and J. Owen, in 'Reports on Progress in Physics' (Ed. A.C. Stickland) Vol. 18, p.304. Published by the Physical Society, London (1955).

13. J.H.E. Griffiths and J. Owen, Proc. Roy. Soc. (London) A213, 459 (1952).

14. B. Bleaney, R.P. Penrose, and B.I. Plumpton, ibid. A198, 406 (1949).

15. D.J.E. Ingram, Proc. phys. Soc. (London) A66, 412 (1953).

16. B. Brovetts, G. Cini, and S. Ferroni, Nuovo Cimento 10, 1325 (1953).

17. B. Bleaney and D.J.E. Ingram, Proc. Roy. Soc. (London) A205, 336 (1951).

18. T. Hayashi and K. Ono, J. phys.Soc. Japan 8, 270 (1953).

19. A.G.H. Dutton, 'Crystallography and Practical Crystal Measurement', Ch. 17, p. 258. Today and Tomorrow Book Agency, New Delhi (1961).

20. R.W. G. Wyckoff, 'Crystal Structures', Vol. 3, p.821. Interscience, New York (1969).

21. W. Hoffmann, Z. Kristallogr. 78, 279 (1931).

22. T.N. Margulis and D.H. Templeton, ibid. 117,344 (1962).

23. L.W. Grimes, H.F. Kay, and M.W. Webb, Acta crystallogr. 16, 823 (1963).

24. D.M.S. Bagguley, B. Bleaney, J.H.E. Griffiths, R.P. Penrose, and B.I. Plumpton, Proc. phys. Soc. (London) 61, 551 (1948).

CHAPTER VI

PARAMAGNETIC RESONANCE OF Mn^{2+} IN NICKEL ACETATE TETRAHYDRATE*

Abstract

Paramagnetic resonance of Mn^{2+} has been studied in nickel acetate tetrahydrate $[Ni(CH_3COO)_2 \cdot 4H_2O]$ at room temperature. The Mn^{2+} ion was found to substitute for Ni^{2+} in the bimolecular unit cell of $Ni(CH_3COO)_2 \cdot 4H_2O$ and exhibit the characteristic magnetic inequivalency. Besides, the Mn^{2+} resonance lines exhibited a direct dependence of the linewidth on the Zeeman-field intensity, and a shift in the g_z value towards the negative side, from the corresponding value for Mn^{2+} in isostructural magnesium acetate tetrahydrate $[Mg(CH_3COO)_2 \cdot 4H_2O]$. These features have been explained in terms of the interaction of Mn^{2+} ion with the Ni^{2+} host ions.

---

* The contents of this chapter, together with a part of the next chapter, have been accepted for publication in J.Chem. Phys.

Introduction:

The most commonly used dilutants, for reducing the interaction between paramagnetic ions, are diamagnetic ions in magnetically dilute mixed crystals.[1] Besides, some paramagnetic ions also were found to act as proper dilutants under certain conditions. Paramagnetic ions whose spin-lattice relaxation time is short at room temperature can be used in place of the diamagnetic ions till high enough temperatures, so that the spin-lattice relaxation time of the diluting ions does not approach the Larmor precession period of the resonating paramagnetic ion.[2,3] Besides, paramagnetic ions whose ground state splitting due to the surrounding crystalline field (ZFS) is much larger than the irradiating microwave frequency, can also be used in place of the diluting diamagnetic ions.[3] The ions which belong to this class are those with even electrons and hence have no Kramers degeneracy, and Ni^{2+} is a good example in the iron group series. The present chapter deals with the EPR studies of Mn^{2+}-doped nickel acetate tetrahydrate $[Ni(CH_3COO)_2 \cdot 4H_2O]$ at room temperature.

Crystal Structure:

The crystal structure of $Ni(CH_3COO)_2 \cdot 4H_2O$ has been determined by van Niekerk and Schoening.[4] The unit cell is monoclinic with

$$a_o = 4.75 \text{ Å}, \quad b_o = 11.77 \text{ Å}, \quad c_o = 8.44 \text{ Å},$$
$$\text{and } \beta = 93^o36',$$

unit contains two molecules related by the operation of the space group $P2_1/c$. For the space group $P2_1/c$, the positions of the atoms are,

$$(0,0,0) \quad \text{and} \quad (0,\tfrac{1}{2},\tfrac{1}{2})$$

for nickel atom, and

$$\pm(x,y,z;x,\tfrac{1}{2}-y,\ z+\tfrac{1}{2})$$

for other atoms and molecules. Each nickel atom is surrounded by a distorted octahedron of four water molecules at distances 2.06 Å and 2.11 Å, and two oxygen atoms of the two acetate groups at 2.12 Å.

The crystals of $Ni(CH_3COO)_2 \cdot 4H_2O$ grow as prismatic needles along the c axis.[5] The projection of the unit cell of $Ni(CH_3COO)_2 \cdot 4H_2O$ along its a_o axis is given in Fig. VI-1.[6]

Results and Discussion:

a. Analysis of the spectra:

The EPR of Mn^{2+} in $Ni(CH_3COO)_2 \cdot 4H_2O$ has been studied at room temperature. The different magnetic complexes were found by studying the angular variation of the resonance spectrum. The z axes of these complexes were obtained by getting the maximum spread of the fine-structure separation. Two fine-structure maxima were obtained corresponding to the two magnetic complexes of Mn^{2+} substituting for Ni^{2+} in the bimolecular unit cell. The two z axes make an angle of $\sim 58^\circ$ with each other and $\sim 60^\circ$ with the crystallographic b axis.

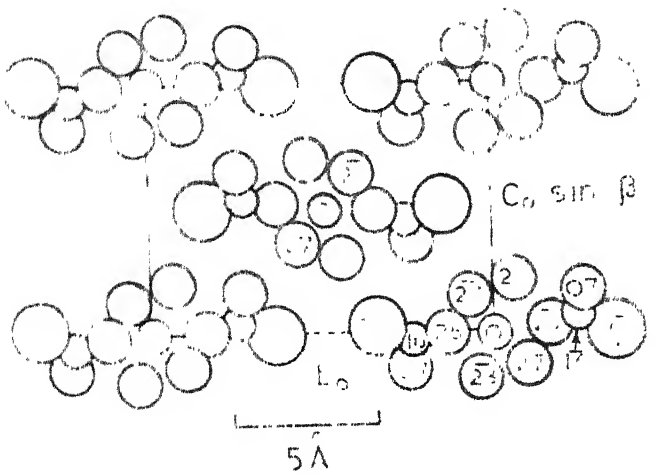

- Ni
- $H_2O(1)$
- $H_2O(2)$
- O (1)
- O (2)
- C
- CH_3

Fig. VI-1 The monoclinic crystal structure of $Ni(CH_3COO)_2 \cdot 4H_2O$ projected along its a_o axis. The numbers inside the circles represent the positions of the atoms or molecule along the a_o axis in units of the unit cell dimension along the a_o axis (100 = 4.75 Å). For the other molecule of the [illegible] of Ni and $H_2O(1)$ are given.

From these observations, it has been concluded that Mn-$H_2O(1)$ forms the z axis of the distorted octahedron of four water molecules and two oxygen atoms surrounding the Mn^{2+} ion substituting for Ni^{2+}.

The EPR spectrum for the Zeeman-field direction along the z axis of one of the magnetic complexes of Mn^{2+} is shown in Fig. VI-2. This has been analyzed for the spin-Hamiltonian constants (as described in Chapter III), and these are,

$g_z = 1.996 \pm 0.005$, $D = +462 \pm 5G$, $A = -90 \pm 5G$,
$|E| = 90 \pm 10G$, and $|B| = 90 \pm 10G$.

b. Effect of Ni^{2+} on the EPR of Mn^{2+}:

As far as the general resonance properties - like the symmetry and the strength of the crystalline field at Mn^{2+}, the angle between the z axes - are concerned, the present system behaves like a system where Mn^{2+} is doped in an isostructural diamagnetic lattice,viz., magnesium acetate tetrahydrate $[Mg(CH_3COO)_2 \cdot 4H_2O]$. In addition, however, a regular increase in the linewidth of Mn^{2+} resonance lines with the Zeeman-field intensity, and a shift in the g_z value towards the negative side, from the corresponding value of Mn^{2+} in isostructural $Mg(CH_3COO)_2 \cdot 4H_2O$, have been observed.

Nickel^{2+} has a $(3d)^8$ outershell configuration and a ground state $^3F_4$. Under an octahedrally coordinated crystalline field, the ground state of this even electron system is orbitally

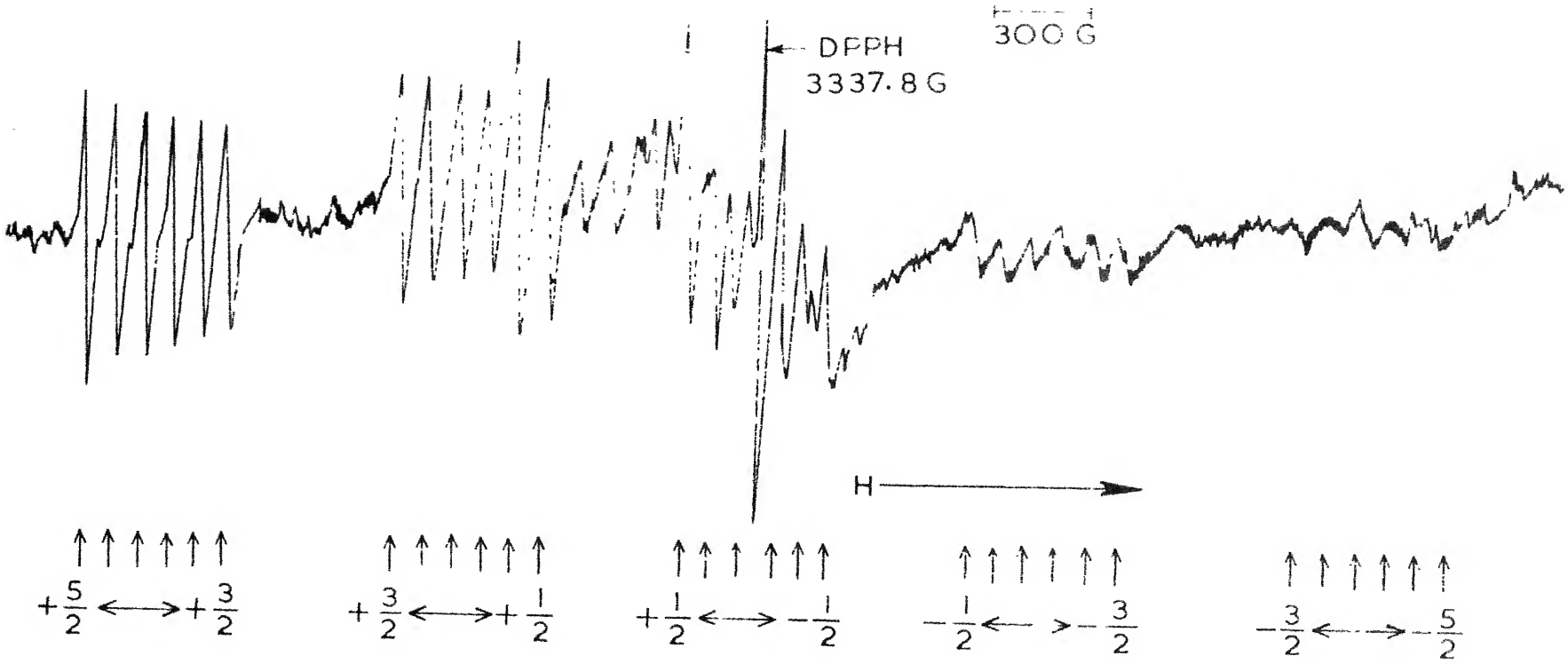

Fig. VI-2: The EPR spectrum of Mn^{2+} in $Ni(CH_3COO)_2 \cdot 4H_2O$ at the Zeeman field [illegible] along the z axis [illegible] of Mn^{2+}.

non-degenerate.[7] Under the action of the crystalline field of orthorhombic or lower symmetry, the spin degeneracy is also removed.[7] The separations between the ground state spin triplet are $|D|-|E|$ and $|2E|$, where D and E are the fine-structure constants for Ni^{2+} in that particular system. These for $Ni(CH_3COO)_2 \cdot 4H_2O$ are,[8]

$$D = -5.61 \text{ cm}^{-1} \quad \text{and} \quad E = -0.83 \text{ cm}^{-1}.$$

These splittings are much larger than the X-band microwave frequency ($\sim 0.3 \text{ cm}^{-1}$) and hence the non-observation of the EPR of Ni^{2+}.

Moriya and Obata[9] have given a detailed account of the effect of paramagnetic ions whose spin is quenched by the crystalline field (like Ni^{2+}, to be referred to as lattice spin), on the EPR of a resonating paramagnetic ion (like Mn^{2+}) introduced in the system. Similar effects relating to the g value have been discussed and observed by Hutchings and Wolf.[10] For these systems when the Zeeman field is set on, magnetic moments are induced on the lattice spins due to polarization effect. This introduces an additional magnetic field at the resonating spin, proportional to the magnitude of the thermal equilibrium value of the lattice spin and the coupling constant between the two spins. The frequency dependence of the fluctuations of this lattice spin, about its thermal equilibrium value, which for the case of Zeeman interaction smaller than the ZFS of the lattice spin, gives rise to the dependence of the

spin-lattice and spin-spin relaxation times of the resonating spin on the Zeeman-field intensity, and hence the linewidth variation of the Mn^{2+} resonance lines with the Zeeman-field intensity.

The magnitude of the g tensor along the z axis, for the present system, is smaller than the free spin g value, while in case of the EPR of Mn^{2+} in isostructural $Mg(CH_3COO)_2 \cdot 4H_2O$,[11] at room temperature, this was observed to be 2.0069, larger than the free spin g value. The positive g shift, from the free spin g value, in the case of Mn^{2+} in $Mg(CH_3COO)_2 \cdot 4H_2O$ has been explained on the basis of the effect of the covalent bonding between the Mn^{2+} ion and the surrounding ligands. $Ni(CH_3COO)_2 \cdot 4H_2O$ is isostructural to $Mg(CH_3COO)_2 \cdot 4H_2O$,[6] and one expects the same magnitude of ZFS of Mn^{2+} in this case also (which is really the case), and a corresponding positive g-shift, from the free spin g value. The negative shift in the g_z value in the case of Mn^{2+} in $Ni(CH_3COO)_2 \cdot 4H_2O$, from that of Mn^{2+} in $Mg(CH_3COO)_2 \cdot 4H_2O$, has been attributed to the polarization effect of Ni^{2+}, which produces a local magnetic field at the Mn^{2+} ion in addition to the Zeeman field. From the shift in g_z value of Mn^{2+} in $Ni(CH_3COO)_2 \cdot 4H_2O$, from the corresponding value for Mn^{2+} in $Mg(CH_3COO)_2 \cdot 4H_2O$, the intensity of the local magnetic field at Mn^{2+} due to Ni^{2+} has been found to be $\sim$ 20 G, for the Zeeman-field direction along the z axis of one of the magnetic complexes.

A best fit calculation has been made of the linewidths of the Mn^{2+} resonance lines (peak-to-peak width of the derivative signal) for linear and quadratic variations with the Zeeman-field intensity, along the z axis of one of the magnetic complexes using the linear regression technique (as described in Chapter III). Due to the overlap of the lines of the second magnetic complex, and the weak intensity of the transitions at larger Zeeman-field intensities, the number of resonance transitions considered for the best fit was limited. The linewidth of the Mn^{2+} resonance transition (ΔH) and the corresponding Zeeman-field intensity (H) considered for the best fit are given in Table VI-1, wherein only well resolved lines have been taken.

TABLE VI-1

The Zeeman-Field Intensity (H) and the Corresponding Linewidth (ΔH) of Mn^{2+} Resonance Lines in $Ni(CH_3COO)_2 \cdot 4H_2O$

H (gauss)	ΔH (gauss)
1285	20.3
1370	21.7
1455	23.7
2212	27.1
2396	31.9
2570	33.9
2660	40.7
4013	47.5
4190	47.5
4478	48.8

The equations used have been,

$$\Delta H = a + bH, \qquad \text{(VI.1)}$$

for the case of linear variation of ΔH with H, and

$$\Delta H = c + dH^2, \qquad \text{(VI.2)}$$

for the case of quadratic variation. The values of these parameters are,

a = 10.0G, b = 0.0091, and the root-mean-square(RMS) deviation = 2.574G,

and c = 21.2G, d = $1.57 \times 10^{-6} G^{-1}$, and RMS = 3.18G.

A brief report of the theory concerning the effect of Ni^{2+} diluting ions on the EPR of Mn^{2+} is given in the Appendix.

REFERENCES

1. B. Bleaney and D.J.E. Ingram, Proc. phys. Soc.(London) A63, 408 (1950).

2. B. Bleaney, R.J. Elliott, and H.E.D. Scovil, ibid. A64, 933 (1951).

3. K. Ono and I. Hayashi, J. phys. Soc. Japan 8, 561 (1953).

4. J.K. van Niekerk and F.R.L. Schoening, Acta crystallogr. 6, 609 (1953).

5. E.W. Porter and R.C. Spiller, 'The Barker Index of Crystals', Vol. 2, W. Heffer and Sons, Cambridge (1956).

6. R.W.G. Wyckoff, 'Crystal Structures,' Vol.5, Interscience, New York (1966).

7. R. Schlapp and W.G. Penney, Phys. Rev. 42, 666 (1932).

8. R.B. Flippen and S.A. Friedberg, ibid. 121,1591 (1961).

9. T. Moriya and Y. Obata, J. phys. Soc. Japan 13,1333 (1958).

10. M.T. Hutchings and W.P. Wolf, Phys. Rev. Lett. 11, 187 (1963).

11. T.J. Manakkil, Ph.D. Thesis, New Mexico State University Las Cruces (1967).

CHAPTER VII

ELECTRON PARAMAGNETIC RESONANCE OF Mn^{2+} IN HEPTAHYDRATED SULFATES OF NICKEL AND MAGNESIUM

Abstract

Electron paramagnetic resonance of Mn^{2+} has been studied in the isostructural single crystals of nickel sulfate heptahydrate ($NiSO_4 \cdot 7H_2O$) and magnesium sulfate heptahydrate ($MgSO_4 \cdot 7H_2O$), at room temperature. The Mn^{2+} ion was found to substitute for the divalent cations in the tetramolecular unit cells of $NiSO_4 \cdot 7H_2O$ and $MgSO_4 \cdot 7H_2O$, and exhibit the characteristic magnetic inequivalency. Besides, the Mn^{2+} resonance lines in $NiSO_4 \cdot 7H_2O$ exhibited a direct dependence of the linewidth on the Zeeman-field intensity, and a shift in the g_z value towards the negative side, from the corresponding value for Mn^{2+} in $MgSO_4 \cdot 7H_2O$. These features have been explained in terms of the interaction of Mn^{2+} ion with the Ni^{2+} host ions.

Introduction:

In studying the EPR of paramagnetic ions, diamagnetic ions are most commonly used as the dilutants in magnetically dilute mixed crystals, so that there is no appreciable interaction between the paramagnetic ions themselves, or with the ions of the diluting medium.[1] There exist certain paramagnetic ions, which can act as proper dilutants under certain conditions. Paramagnetic ions whose spin-lattice relaxation time is short at room temperature can be used as dilutants till high enough temperatures, so that the spin-lattice relaxation time of the diluting ion does not approach the Larmor precession period of the resonating paramagnetic ion.[2,3] Besides, paramagnetic ions whose ZFS is much larger than the irradiating microwave frequency, can also be used as dilutants.[3] The ions which belong to the second class are those with even number of unpaired electrons, and hence have no Kramers degeneracy. In a crystalline field of lower-than-axial symmetry the orbital and spin degeneracies are completely removed, by the combined action of the crystalline-field and spin-orbit interactions. Divalent nickel is a good example of this class of paramagnetic ions in the iron group series. In Chapter VI we have dealt with the EPR of Mn^{2+} in one of the nickel compounds, viz., $Ni(CH_3COO)_2 \cdot 4H_2O$. The present chapter is an extension of the similar type of study in nickel sulfate heptahydrate ($NiSO_4 \cdot 7H_2O$), at room temperature. For a comparative study, the EPR of Mn^{2+} in

isostructural magnesium sulfate heptahydrate ($MgSO_4 \cdot 7H_2O$) has also been studied at room temperature.

Crystal Structure:

$NiSO_4 \cdot 7H_2O$ and $MgSO_4 \cdot 7H_2O$ are isostructural,[4] with orthorhombic unit cell symmetry. The crystal structure of $NiSO_4 \cdot 7H_2O$ has been determined by Beevers and Schwartz.[5] The unit cell is tetramolecular, the four molecules being related by the operation of the space group $P2_12_12_1$. The unit cell dimensions are,[4]

for $NiSO_4 \cdot 7H_2O$:

$$a_o = 11.86 \text{ Å}, \quad b_o = 12.08 \text{ Å}, \quad \text{and} \quad c_o = 6.81 \text{ Å},$$

and for $MgSO_4 \cdot 7H_2O$:

$$a_o = 11.91 \text{ Å}, \quad b_o = 12.02 \text{ Å}, \quad \text{and} \quad c_o = 6.87 \text{ Å}.$$

For the space group operation $P2_12_12_1$, the atoms and molecules are in the positions

$$(x,y,z;\ \bar{x},\bar{y},z+\tfrac{1}{2};\ x+\tfrac{1}{2},\tfrac{1}{2}-y,\bar{z};\ \tfrac{1}{2}-x,y+\tfrac{1}{2},\tfrac{1}{2}-z).$$

Each divalent cation is surrounded by six water molecules, $[H_2O(1)-H_2O(6)]$, at distances ranging from, in the case of $NiSO_4 \cdot 7H_2O$, 1.93 Å - 2.40 Å. The seventh water molecule, $H_2O(7)$, is not coordinated with a cation, but instead fills what would otherwise be a hole in the structure.

The single crystals of $NiSO_4 \cdot 7H_2O$ and $MgSO_4 \cdot 7H_2O$ grow as prismatic needles along the c axis.[6] The projection of the

unit cell of $NiSO_4 \cdot 7H_2O$ along its c_o axis is shown in Fig. VII-1.

Results and Discussion:

a. Analysis of the spectra:

The EPR of Mn^{2+} in $NiSO_4 \cdot 7H_2O$ and $MgSO_4 \cdot 7H_2O$ has been studied at room temperature. Hayashi and Ono[7] have studied the EPR of Mn^{2+} in $MgSO_4 \cdot 7H_2O$, but the constants were not reported accurately. We have studied the system once again and determined the constants accurately, for comparison with the results on Mn^{2+}-doped $NiSO_4 \cdot 7H_2O$. The different complexes of Mn^{2+} in $NiSO_4 \cdot 7H_2O$ and $MgSO_4 \cdot 7H_2O$ were found by studying the angular variation of the resonance spectrum. The z axes of these complexes were obtained by getting the maximum spread of the fine-structure separation. Four fine-structure maxima were obtained corresponding to the four magnetic complexes of Mn^{2+} substituting for Ni^{2+} and Mg^{2+}. The z axis of each Mn^{2+} complex in $NiSO_4 \cdot 7H_2O$ makes angles of $\sim 32^\circ$, 55°, and 55° with the z axes of the other three complexes. This coincides fairly closely with the supposition that the z axis of the distorted octahedron of six water molecules is along the line joining manganese and the water molecule at shortest distance from nickel, viz., $H_2O(3)$.

The EPR spectra of Mn^{2+} in $NiSO_4 \cdot 7H_2O$ and $MgSO_4 \cdot 7H_2O$, for the Zeeman-field direction along the z axis of one of the magnetic complexes, are shown in Figs. VII-2 and 3, respectively. These have been analyzed for the spin-Hamiltonian constants

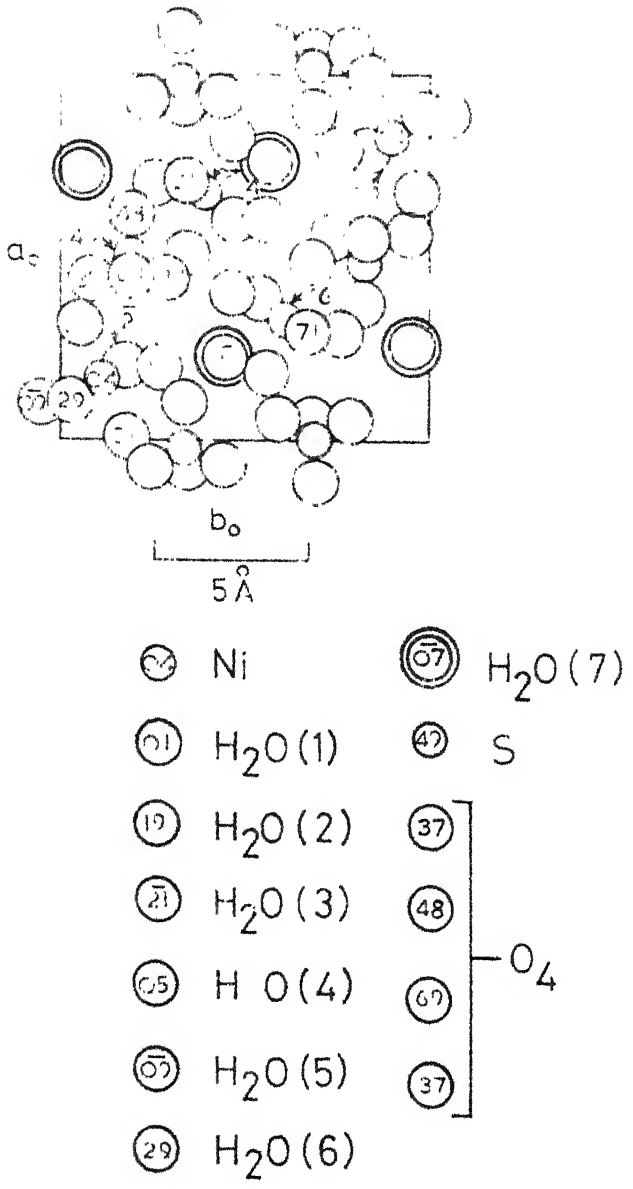

Fig. VII-1. The orthorhombic crystal structure of $NiSO_4 \cdot 7H_2O$ projected along its c_o axis. The numbers inside the circles represent the positions of the atoms or molecules along the c_o axis in units of the unit cell dimension along the c_o axis (100 = 6.81 Å). The seventh H_2O, which is not coordinated to the nickel atom, is doubly ringed. For the other molecules the positions of Ni and $H_2O(5)$ are given.

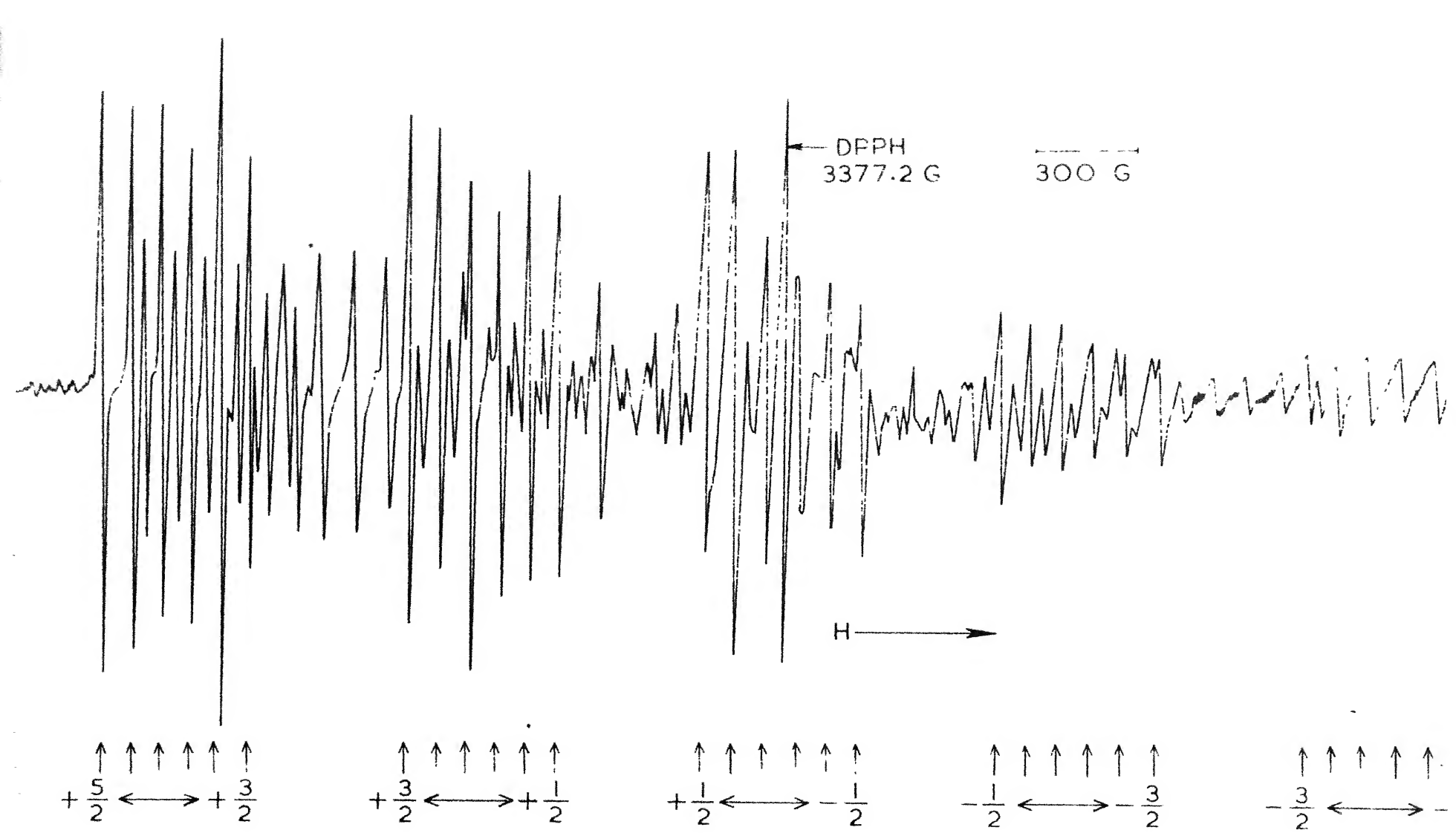

Fig. VII-2: The EPR spectrum of Mn^{2+} in $MnSO_4 \cdot H_2O$ [illegible] the Zeeman-[illegible] the [illegible] of one of the [illegible] of Mn^{2+}.

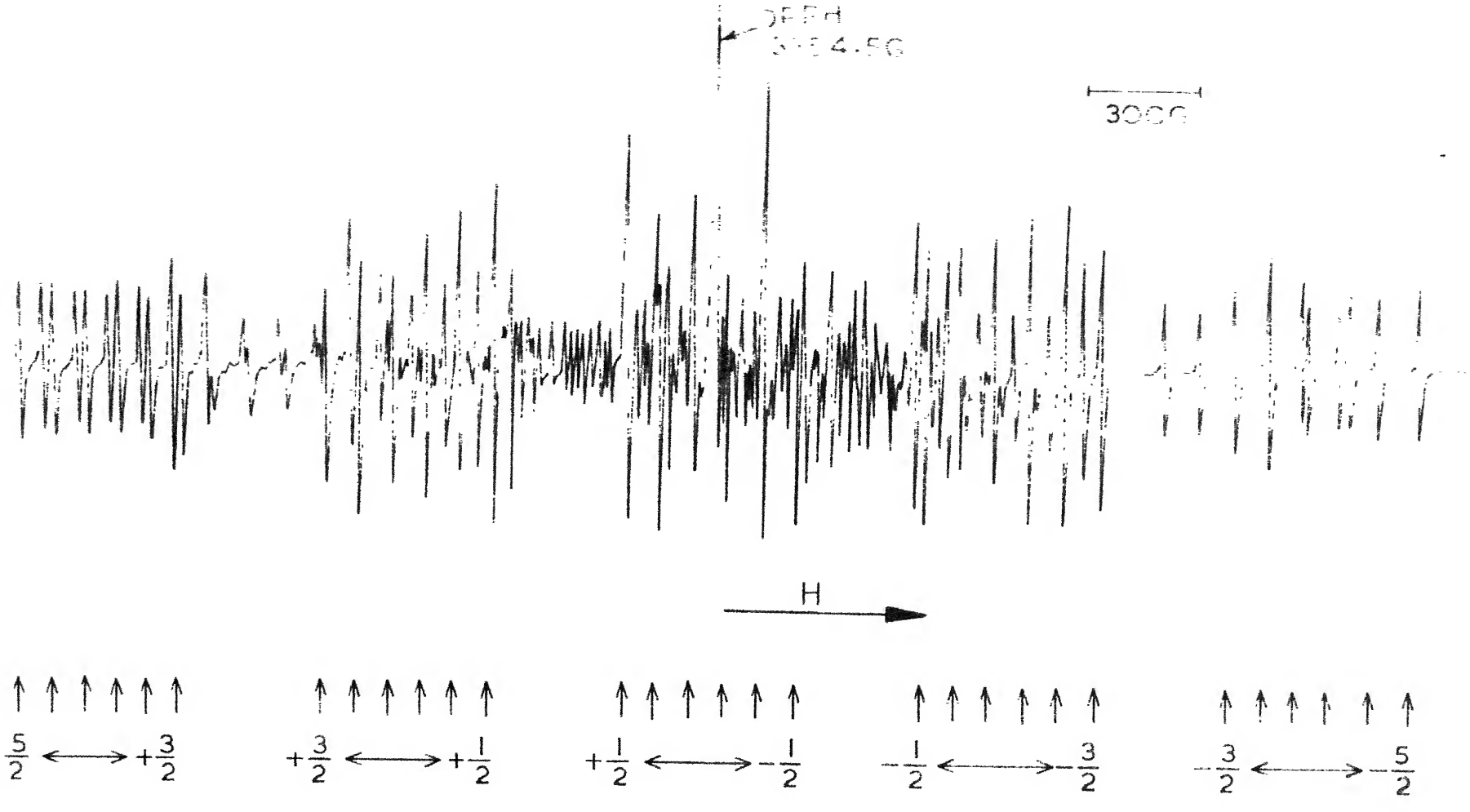

Fig. VII-1 The EPR spectrum of Mn^{2+} in $MgSO_4 \cdot 7H_2O$ for the Zeeman-field direction along the z axis of one of the magnetic complexes of Mn^{2+}.

(as described in Chapter III), which are,

for Mn^{2+} in $NiSO_4 \cdot 7H_2O$:

$g_z = 1.995 \pm 0.005$, $D = +448 \pm 5G$, $A = -91 \pm 5G$,
$|E| = 74 \pm 10G$, and $|B| = 87 \pm 10G$,

and for Mn^{2+} in $MgSO_4 \cdot 7H_2O$:

$g_z = 2.003 \pm 0.005$, $D = +412 \pm 5G$, $A = -92 \pm 5G$,
$|E| = 95 \pm 10G$, and $|B| = 87 \pm 10G$.

The crystal-field parameters D and E in the two systems are very nearly the same, indicating that the configuration of water molecules at Ni^{2+} and Mg^{2+} is very nearly same. The observed differences may be due to small differences in the distances of the water molecules from the cations in the two cases.

b. Effect of Ni^{2+} on the EPR of Mn^{2+}:

As far as the general resonance properties - like the symmetry and the strength of the crystalline field at Mn^{2+}, the angle between the axes - are concerned, both the systems, $NiSO_4 \cdot 7H_2O$ and $MgSO_4 \cdot 7H_2O$, behave in the same manner. In addition, in the case of Mn^{2+} in $NiSO_4 \cdot 7H_2O$, we have observed a regular increase in the linewidth of Mn^{2+} resonance lines with the Zeeman-field intensity, and a shift in the g_z value towards the negative side, from the corresponding value for Mn^{2+} in $MgSO_4 \cdot 7H_2O$.

The ground state spin triplet of Ni^{2+} in an octahedral crystalline field, under the combined action of crystalline field of lower-than-axial symmetry and spin-orbit interaction, has its spin degeneracy completely removed.[8] The separations between the components of the ground state triplet are $|D| - |E|$ and $|2E|$, where D and E are the fine-structure constants of Ni^{2+} in that particular system. For Ni^{2+} in $NiSO_4 \cdot 7H_2O$ these are,[9]

$$D = -3.56 \text{ cm}^{-1} \quad \text{and} \quad E = -1.5 \text{ cm}^{-1}.$$

These splittings are much larger than the X-band microwave frequency ($\sim$0.3 cm^{-1}) and hence the non-observation of the EPR of Ni^{2+}.

The effect of lattice spin, for the case where the spin angular momentum is completely quenched, on the EPR of Mn^{2+} introduced in that system has been studied detailedly by Moriya and Obata,[10] and the effects relating to the g value have been discussed and observed by Hutchings and Wolf.[11] For these systems, when the Zeeman field is set on, magnetic moments are induced on the lattice spins, due to polarization effect. This introduces an additional magnetic field at the resonating spin (Mn^{2+}), proportional to the magnitude of the thermal equilibrium value of the lattice spin and the coupling constant between the resonating and lattice spins. The frequency dependence of the fluctuations of this lattice spin, about its thermal equilibrium value, which for the Zeeman interaction

smaller than the EPS of the lattice spin, gives rise to the dependence of the spin-lattice and spin-spin relaxation times of the resonating spin on the Zeeman-field intensity. Hence the linewidths of Mn^{2+} resonance lines exhibit a direct dependence on the Zeeman-field intensity. From the observed g_z shift in the case of Mn^{2+} in $NiSO_4 \cdot 7H_2O$, from the corresponding value for Mn^{2+} in isostructural $MgSO_4 \cdot 7H_2O$, it has been possible to calculate the intensity of the additional magnetic field at Mn^{2+} due to Ni^{2+} in $NiSO_4 \cdot 7H_2O$. Assuming that the g_z-shift is entirely due to the effect of Ni^{2+}, the additional magnetic field is $\sim$15G at Mn^{2+}, for the Zeeman-field direction along the z axis of that complex.

A best fit calculation has been made of the linewidths of the Mn^{2+} resonance lines (peak-to-peak width of the derivative signal) for linear and quadratic variations with the Zeeman-field intensity along the z axis of a magnetic complex. The method used has been the linear regression theory (described briefly in Chapter III). Only those transitions whose lines are clearly resolved have been considered for the best fit, and some representative values of these are given in Table VII-1.

TABLE VII-1

The Zeeman-Field Intensity (H) and the Corresponding Linewidth (ΔH) of Mn^{2+} Resonance Lines in $NiSO_4 \cdot 7H_2O$.

H (gauss)	ΔH (gauss)
2510	13.1
3122	16.5

...contd...

3569	18.1
4448	20.3
5166	21.6
5266	22.0

Eqs. (VI.1) and (VI.2) were used for the best fit calculation, and the parameters obtained are,

$$a = 6.51G, \quad b = 3.0\times10^{-3}, \quad \text{and} \quad RMS = 0.63G,$$

and $$c = 16.89G, \quad d = 0.1\times10^{-6}G^{-1} \text{ and } RMS = 2.34G.$$

A brief report of the theory concerning the effect of Ni^{2+} diluting ions on the EPR of Mn^{2+} is given in the Appendix.

REFERENCES

1. B. Bleaney and D.J.E. Ingram, Proc. phys. Soc. (London) A63, 408 (1950).

2. B. Bleaney, R.J. Elliott, and H.E.D. Scovil, ibid. A64, 933 (1951).

3. K. Ono and I. Hayashi, J. phys. Soc. Japan 8, 561 (1953).

4. R.W.G. Wyckoff, 'Crystal Structures', Vol. 3, p.839. Interscience, New York (1965).

5. C.A. Beevers and C.M. Schwartz, Z. kristallogr. 91A, 157 (1935).

6. M.W. Porter and R.C. Spiller, 'The Barker Index of Crystals', Vol. 1, W. Heffer and Sons, Cambridge (1951).

7. I. Hayashi and K. Ono, J. phys. Soc. Japan 8, 270 (1953).

8. R. Schlapp and W.G. Penney, Phys. Rev. 42, 666 (1932).

9. K. Ono, J. phys. Soc. Japan 8, 802 (1953).

10. T. Moriya and Y. Obata, ibid. 13, 1333 (1958).

11. M.T. Hutchings and W.P. Wolf, Phys. Rev. Lett. 11, 187 (1963).

APPENDIX

EFFECT OF Ni^{2+} DILUTING IONS ON THE EPR OF Mn^{2+}

Chapters VI and VII describe the EPR of Mn^{2+} in single crystals of Ni^{2+} salts, and the results therein have been interpreted on the basis of the theoretical study by Moriya and Obata.[1] Here a brief summary of their work is presented.

The $(3d)^8$ configuration of Ni^{2+} in an octahedrally coordinated crystalline field has an orbital singlet as its ground state.[2] The spin degeneracy is also removed completely in the presence of a crystalline field of lower-than-axial symmetry, by the combined action of the crystalline field and spin-orbit interactions.[2] Thus, in such an environment, both the orbital and spin angular momenta are completely quenched for the ground state of the Ni^{2+} ion. In such a case the diagonal component (low-frequency component) of the ground state magnetic moment is zero, in the absence of the externally applied Zeeman field, and the Ni^{2+} ion is nonmagnetic. When the Zeeman field (H) is set on, magnetic moments are induced on this nonmagnetic state, because of the matrix elements connecting the ground state, $|0\rangle$ and the high-lying electronic

1. T. Moriya and Y. Obata, J. phys. Soc. Japan 13, 1333 (1958).
2. R. Schlapp and W.G. Penney, Phys. Rev. 42, 666 (1932).

states, $|n\rangle$, (high-frequency component of the magnetic moment), due to the polarization effect. The induced magnetic moment is proportional to H and $|\langle n|M|0\rangle|^2$, where M is the magnetic moment operator along the Zeeman-field direction.[3] Since the low-frequency component is zero we have

$$W_1 = 0 \qquad (A.1)$$

in Eq. (II.22), and hence the energy of this system can be written, upto second order in H, as

$$E = W_0 + W_2 H^2$$

$$= W_0 + \sum_\mu W_{2\mu} H_\mu^2. \qquad (A.2)$$

Moriya and Obata[1] have discussed the EPR of a resonating spin (Mn^{2+}) introduced in a salt where the Ni^{2+} are the diluting ions, and the effect of Ni^{2+} on the EPR of Mn^{2+}. At temperatures (T) such that $kT < \Delta$ $(=E_n - E_0)$, the thermal equilibrium value of the Ni^{2+} spin is given as

$$\langle S_\mu \rangle = \sum_m f_m (S_\mu)_{mm}. \qquad (A.3)$$

m is the summation over the various spin states of the Ni spin an

f_m is the statistical factor given by

$$f_m = \exp(-E_m/kT)/\sum_m \exp(-E_m/kT), \qquad (A.4)$$

and $(S_\mu)_{mm}$ are the diagonal elements of the μ-th component of the Ni^{2+} spin. Then the spin S of Ni^{2+} can be written as the

3. C. Kittel, 'Introduction to Solid State Physics', App.E, p.578, Asia Publishing House, Lucknow (1966).

contribution of two terms as

$$S = \langle S \rangle + \delta S, \qquad (A.5)$$

where δS is the fluctuation of the spin from its thermal equilibrium value.

Now we consider the Hamiltonian of the Mn^{2+} ion, with the effect of the Ni^{2+} ion on it. This is written as

$$\mathcal{H} = \mathcal{H}_{Mn} + \mathcal{H}_{Mn-Ni}, \qquad (A.6)$$

where $\mathcal{H}_{Mn}$ is the Zeeman term in the spin Hamiltonian of Mn^{2+}, and

$$\mathcal{H}_{Mn-Ni} = \text{constant} \times \sum_{\nu=1}^{3} \mathcal{S}_{\nu} \sum_{j\mu} \phi_j^{\nu\mu} S_{j\mu}, \qquad (A.7)$$

$\mathcal{S}_{\nu}$ is the ν-th component of the Mn^{2+} spin, $\phi_j^{\nu\mu}$ is the coupling constant between Mn^{2+} and Ni^{2+} spins, like the dipolar or exchange coupling, and $S_{j\mu}$ is the μ-th component of the j-th Ni^{2+} spin, where more than one Ni^{2+} ion are contributing to $\mathcal{H}_{Mn-Ni}$. Eq. (A.6) is written as

$$\mathcal{H} = \mathcal{H}_0 + \mathcal{H}', \qquad (A.8)$$

where

$$\mathcal{H}_0 = g\beta(\vec{H} + \text{constant} \times \sum_{\nu\mu} \phi_j^{\nu\mu} S_{j\mu}) \cdot \vec{\mathcal{S}} \qquad (A.9)$$

and

$$\mathcal{H}' = \text{constant} \times (\sum_{\nu j\mu} \phi_j^{\nu\mu} S_{j\mu}) \cdot \vec{\mathcal{S}}. \qquad (A.10)$$

The thermal equilibrium value of the Ni^{2+} spin produces an additional field at Mn^{2+}, proportional to $\phi_j^{\nu\mu}$ and $\langle S_{j\mu} \rangle$, Eq. (A.9), in addition to the Zeeman field. This additional field results in the g-shift, which has been calculated from the g value of the EPR of Mn^{2+} in an isostructural, diamagnetic salt.

The effect of the fluctuations of the Ni^{2+} spin is obtained by considering the effect of $\mathcal{H}'$ on $\mathcal{H}_0$. This has been done by considering the motional effect, with the combination coming from the secular and non-secular effects.[4] This leads to the dependence of $1/T_1$ and $1/T_2$ on $\langle \delta S_\mu(t) \delta S_\nu \rangle$, where T_1 and T_2 are the spin-lattice and spin-spin relaxation times of Mn^{2+}, and

$$\delta S_\mu(t) = \exp(it\mathcal{H}_{Ni}/h)\delta S_\mu \exp(-it\mathcal{H}_{Ni}/h). \qquad (A.11)$$

$\langle \delta S_\mu(t) \delta S_\nu \rangle$ is further related to the difference between the isothermal and isolated susceptibilities (χ_T and χ_{is}) in the following way.

$$\langle \delta S_\mu(t) \delta S_\nu \rangle = \sum_n G_{\mu\nu}^{(n)}(t), \qquad (A.12)$$

where $G_{\mu\nu}^{(n)}(t)$ is the 'auto-moment' of the Ni^{2+} spin.

---

4. R. Kubo and K. Tomita, J. phys. Soc. Japan 9, 888 (1954).

$$G_{\mu\nu}^{(0)}(t) = \langle (S_\mu)_{mm}(S_\nu)_{mm} \rangle - \langle S_\mu \rangle \langle S_\nu \rangle \qquad (A.13)$$

and hence

$$g_\mu^2 g_\nu^2 \beta^2 G_{\mu\nu}^{(0)}(t) = \left\langle \frac{\partial E}{\partial H_\mu} \frac{\partial E}{\partial H_\nu} \right\rangle - \left\langle \frac{\partial E}{\partial H_\mu} \right\rangle \left\langle \frac{\partial E}{\partial H_\nu} \right\rangle$$

$$= kT(\chi_T - \chi_{is})_{\mu\nu} , \qquad (A.14)$$

where g_μ, g_ν are the μ-th and ν-th components of the g value of the Ni^{2+} ion in that particular compound. Since E is given by Eq. (A.9), we have

$$kT(\chi_T - \chi_{is})_{\mu\nu} = 2(\langle W_{2\mu} W_{2\nu} \rangle - \langle W_{2\mu} \rangle \langle W_{2\nu} \rangle) H_\mu H_\nu , \qquad (A.15)$$

a function of the Zeeman-field intensity. Thus $1/T_1$ and $1/T_2$, and hence the widths of Mn^{2+} resonance lines, exhibit a direct dependence on the Zeeman-field intensity.

The results that have been obtained in the EPR of Mn^{2+} in the two Ni^{2+} salts (Chapters VI and VII) are in confirmity with these predictions of the theory of Moriya and Obata.[1]

PHY-1970-D-JAN-LL